Inactivation of the cytoprotective major vault protein by caspase-1 and -9 in epithelial cells during apoptosis

Serena Grossi, Gabriele Fenini, Tobias Kockmann, Paulina Hennig, Michela Di Filippo, Hans-Dietmar Beer

PII: S0022-202X(19)33499-2

DOI: https://doi.org/10.1016/j.jid.2019.11.015

Reference: JID 2231

To appear in: *The Journal of Investigative Dermatology*

Received Date: 13 June 2019

Revised Date: 7 November 2019

Accepted Date: 8 November 2019

Please cite this article as: Grossi S, Fenini G, Kockmann T, Hennig P, Di Filippo M, Beer H-D, Inactivation of the cytoprotective major vault protein by caspase-1 and -9 in epithelial cells during apoptosis, *The Journal of Investigative Dermatology* (2020), doi: https://doi.org/10.1016/j.jid.2019.11.015.

Inactivation of the cytoprotective major vault protein by caspase-1 and -9 in epithelial cells during apoptosis

Serena Grossi[1,2], Gabriele Fenini[1,2], Tobias Kockmann[3], Paulina Hennig[1,2], Michela Di Filippo[1,2], Hans-Dietmar Beer[1,2*]

1. Department of Dermatology, University Hospital Zurich, Gloriastrasse 31, F floor, CH-8091 Zurich, Switzerland
2. Faculty of Medicine, University of Zurich, Zurich, Switzerland
3. Functional Genomics Center Zurich, ETH Zurich / University of Zurich, Winterthurerstrasse 190, Y32H92b, CH-8057 Zurich, Switzerland

Keywords: keratinocytes, UVB, inflammasome, apoptosis

Short title: caspase-1 and -9 inactivate the major vault protein

* Correspondence and requests for materials should be addressed to H.D.B. (email: Hans-Dietmar.Beer@usz.ch; phone: +41 44 25 53 97 3; Gloriastrasse 31,CH- 8091 Zurich, Switzerland)

ABSTRACT

Inflammasome activation induces caspase-1-dependent secretion of the proinflammatory cytokine IL-1β. In addition, caspase-1 activates gasdermin D (GSDMD) in immune cells causing pyroptosis, a lytic type of cell death. In contrast, UVB irradiation of human primary keratinocytes (HPKs) induces NLRP1 inflammasome activation, cytokines secretion and caspase-1-dependent apoptosis, rather than pyroptosis. Here, we addressed the molecular mechanisms underlying the role of caspase-1 in UVB-induced cell death of HPKs. We show that GSDMD is a poor substrate of caspase-1 in HPKs and that its activation upon UVB irradiation supports secretion of IL-1β. We screened for novel substrates of caspase-1 by a mass spectrometry-based approach and identified the specific cleavage of major vault protein (MVP) at D441 by caspase-1 and -9. MVP is the main component of vaults, highly conserved ribonucleoprotein particles, whose functions are poorly understood. Cleavage of MVP is a common event occurring in HPKs and fibroblasts undergoing apoptosis induced by different stimuli. In contrast, MVP cleavage could not be detected in pyroptotic cells. Cleavage of MVP by caspase-1/-9 inactivates this cytoprotective protein. These results demonstrate a pro-apoptotic activity of caspase-1 and a crosstalk with caspase-9 upon inactivation of the cytoprotective MVP in apoptotic epithelial cells.

INTRODUCTION

Apoptosis is a type of programmed cell death required for development and homeostasis of multicellular organisms. Caspases, a group of aspartate-specific cysteine proteases, play key roles in the induction and execution of cell death including apoptosis (Kaufmann and Hengartner, 2001). They are initially expressed as enzymatically inactive pro-proteins and their activation is tightly regulated. In addition to cell death, several other functions of caspases were identified (Bell and Megeney, 2017, Nakajima and Kuranaga, 2017).

Caspase-1 is a central regulator of inflammation. It cleaves and thereby activates the pro-inflammatory cytokines prointerleukin(IL)-1β and -18 which induce inflammation upon release (Dinarello, 2009). Sensing of many different stresses, including endogenous damage- and exogenous pathogen-associated molecular patterns, induces assembly of protein complexes termed inflammasomes (Broz and Dixit, 2016). Canonical inflammasomes consist of a sensor protein, such as NOD-like receptor (NLR), pyrin domain-containing-1 (NLRP1), NLRP3 or absent in melanoma 2 (AIM2), the adaptor apoptosis-associated speck-like protein containing a caspase recruitment domain (ASC) and caspase-1. The latter is activated upon inflammasome assembly (Broz and Dixit, 2016). Inflammasome activation plays a central role in immunity but contributes also to numerous inflammatory diseases (Strowig et al., 2012). In immune cells, inflammasome and caspase-1 activation cause a lytic pro-inflammatory type of cell death termed pyroptosis. Pyroptosis is induced upon cleavage and activation of gasdermin D (GSDMD) by either caspase-1 or by the inflammatory caspase-4 and -5 (or caspase-11 in mice) after non-canonical inflammasome activation (Kayagaki et al., 2015, Shi et al., 2015). The N-terminal fragment of GSDMD oligomerizes and forms pores in the extracellular membrane, allowing release of IL-1β and -18 (Ding et al., 2016, Liu et al., 2016). In addition, GSDMD pores cause cell lysis by swelling and subsequent disruption of the cell. Therefore, in contrast to apoptotic caspases, activation of inflammatory caspases in certain types of

immune cells is linked to pyroptosis. However, in the absence of GSDMD, caspase-1 can also induce apoptosis (Taabazuing et al., 2017, Tsuchiya et al., 2019).

Keratinocytes are the main cell type of the epidermis, a stratified constantly renewing epithelium, which exerts an essential barrier function against exogenous insults (Fuchs and Raghavan, 2002). UVB irradiation of cultured human but not murine keratinocytes induces NLRP1-dependent inflammasome activation and secretion of IL-1β (Feldmeyer et al., 2007, Fenini et al., 2018b, Sand et al., 2018), suggesting that this process underlies sunburn induction in human (Faustin and Reed, 2008). Recently, a critical role of NLRP1 in human skin was indeed demonstrated (Grandemange et al., 2017, Zhong et al., 2016). Activating mutations of NLRP1 cause inflammatory skin conditions and predispose to skin cancer development (Zhong et al., 2016). In addition, SNPs in the *NLRP1* gene are associated with major inflammatory and autoimmune diseases of the skin, such as psoriasis and vitiligo (Jin et al., 2007a, Jin et al., 2007b, Levandowski et al., 2013).

UVB-irradiated human primary keratinocytes (HPKs) secrete IL-1β by an incompletely understood process, termed unconventional protein secretion, which is regulated by caspase-1 (Keller et al., 2008). UVB is a classical inducer of apoptosis (Salucci et al., 2012) and HPKs undergo UVB-induced apoptosis several hours after inflammasome activation and cytokine secretion in a caspase-1-dependent manner (Sollberger et al., 2015). As skin cancer is mainly caused by UVB radiation and antagonized by apoptosis, UVB-induced apoptosis of HPKs is a highly relevant process.

Here, we characterized the role of caspase-1 activity in UVB-induced apoptosis of HPKs. Although expressed, GSDMD is not efficiently activated by caspase-1 in these cells. Instead, we identified the cytoprotective major vault protein (MVP) (Steiner et al., 2006) as a substrate of caspase-1 and -9 in UVB-irradiated HPKs, but also in other epithelial cells undergoing apoptosis. Our results suggest that caspase-dependent inactivation of MVP facilitates cell death. These findings support the concept of an involvement of caspase-1 in apoptosis.

RESULTS

GSDMD is not efficiently activated by caspase-1 in UVB-irradiated HPKs

As a possible role of GSDMD in HPKs has never been addressed, we analyzed GSDMD expression and processing in this cell type (Figure 1). GSDMD protein was expressed by HPKs (Figure 1 a-c). When HPKs underwent apoptosis 24 hours after UVB irradiation (Sollberger et al., 2015) or upon treatment with staurosporine, GSDMD was processed, leading to generation of a fragment with a molecular weight between 30 and 53 kDa (Figure 1a). This processing was also reported to occur during apoptosis in other cell types and most likely reflects inactivation of GSDMD (Taabazuing et al., 2017). However, in contrast to inflammasome-activated THP-1 cells, we detected only low amounts of the active pore-forming N-terminal p30 fragment of GSDMD upon caspase-1 activation by either UVB radiation or treatment with talabostat, an anti-tumor drug activating the NLRP1 inflammasome (Okondo et al., 2017, Okondo et al., 2018) (Figure 1a). Furthermore, transfection of LPS, which causes activation of caspase-4 in human keratinocytes (Shi et al., 2014), did not result in major GSDMD activation. Even upon overexpression of wild-type caspase-1 in HPKs (Figure 1b), we detected a strong reduction of the level of full-length (p53) GSDMD which most likely represents its degradation rather than its activation. To further determine the function of GSDMD in HPKs we knocked down its expression upon transfection of two different siRNAs (Figure 1c and Supplementary Figure S10). In contrast to control HPKs, mature IL-1β accumulated in these cells 6 hours after UVB irradiation, whereas the amounts of the cytokine in the supernatant were significantly lower at this time point. In addition, we detected more cleaved caspase-3 in GSDMD knockdown HPKs and less LDH release. These experiments suggest a role of GSDMD in unconventional secretion of IL-1β by HPKs. In immune cells, inflammatory caspases activate GSDMD and in turn induce pyroptosis. In contrast, activation of caspases in HPKs results in formation of only low

amounts of the pore-forming N-terminal fragment of GSDMD and/or in its degradation. Furthermore, our findings confirm that living HPKs secrete IL-1β upon UVB irradiation and undergo apoptosis several hours after inflammasome activation (Sollberger et al., 2015).

A mass spectrometry approach identifies major vault protein (MVP) as a substrate of caspase-1

The fact that caspase-1 activity is required for UVB-induced apoptosis of HPKs (Sollberger et al., 2015) suggests the existence of unknown substrates of the protease, involved in this process. Overnight overexpression of wild-type (wt) caspase-1 in HPKs caused activation of the well-established substrate proIL-1β and the release of the mature cytokine into the medium (Figure 1b). In addition, cells died by apoptosis reflected by activation of caspase-3 (Figure 1b) without the need of an additional stimulus. For the identification of novel caspase-1 substrates, we used a mass spectrometry-based approach, tandem mass tag (TMT) terminal amine isotopic labeling of substrates (TAILS) (Kleifeld et al., 2010, Kleifeld et al., 2011) and compared the N-terminomes of HPKs overexpressing in an inducible manner either carboxy-terminal FLAG-tagged wt caspase-1, the enzymatically inactive C285A mutant (mut) or eGFP (used as a control) (Figure 2a). The identified N-terminal peptides were filtered for those cleaved after an aspartate (D), the typical caspase cleavage site. This led to identification of the major vault protein (MVP) as a potential caspase-1 substrate (Figure 2b and c), cleaved at position 441 (Figure 2d) in HPKs upon overexpression of wt caspase-1, but not the inactive mutant or eGFP (Figure 2c).

MVP is an ubiquitously expressed 892 amino acid protein (Berger et al., 2009) and is the main component of large ribonucleoprotein particles termed vaults (van Zon et al., 2003). These organelles have an open barrel-shaped structure, are evolutionary conserved and widely expressed by different species (Kedersha et al., 1990). It has been suggested that vaults are involved in transport processes, immunity, drug resistance of cancer cells, cell death

susceptibility or/and act as signaling platforms (Berger et al., 2009, Kowalski et al., 2007, Ryu et al., 2008, Scheffer et al., 2000, Teng et al., 2017).

Cleavage of MVP in the cell lysates used for the N-terminome analysis was confirmed by immunoblotting using two different MVP-specific antibodies (Figure 2e), recognizing either the amino-terminus (α-MVP (NT)) or the carboxy-terminus (α-MVP (CT)) of MVP (Supplementary Figure S1). Both the N- and the C-terminal fragments of MVP (p53 and p54, respectively) were detected (Figure 2e).

Caspase-1 and caspase-9 cleave MVP

In order to confirm cleavage of MVP by caspase-1 and test whether other caspases are able to target the protein, we incubated recombinant purified MVP with active p20/p10 tetramer of different apoptotic caspases, including caspase-1 (Figure 3a). Caspase-1 was able to cleave MVP, whereas caspase-3, caspase-7, caspase-8, caspase-10 and caspase-2 were ineffective. Interestingly, also active recombinant caspase-9 cleaved MVP *in vitro* (Figure 3a). Moreover, MVP cleavage was also observed upon incubation with recombinant caspase-6 (Figure 3a); however, the pattern of generated MVP fragments was different compared to the one obtained upon incubation with recombinant caspase-1 and -9. Thus, caspase-1 and the apoptotic initiator caspase-9 are able to process MVP in a similar manner *in vitro*. This finding was confirmed upon overexpression of MVP and full-length caspase-1 or -9 in HEK293T cells (Figure 3b).

Furthermore, we tested whether other inflammatory caspases are able to cleave MVP by overexpressing either wild-type caspase-1, caspase-4, caspase-5, or their enzymatically inactive mutants, with MVP. As positive control for the activity of the caspases, we overexpressed proIL-1β. All wild-type caspases were able to cleave proIL-1β and caspase-1 was the most efficient one. However, in contrast to GSDMD, which is activated by all inflammatory caspases (Shi et al., 2015), MVP was only processed by caspase-1 (Figure 3c).

Mass spectrometry analysis revealed D441 as the caspase cleavage site of MVP (Figure 2d). In order to confirm this finding, we co-expressed wild-type MVP or two MVP mutants lacking D441, MVP(D441A) and MVP(D441E), together with caspase-1. In contrast to wild-type MVP, both D441 mutants were cleavage-resistant, confirming this residue as MVP specific cleavage site (Figure 3d).

In conclusion, caspase-1 and the apoptotic initiator caspase-9 are able to cleave MVP specifically at D441 *in vitro* and upon overexpression.

MVP cleavage in apoptotic keratinocytes and fibroblasts requires caspase-1/-9

Then, we analyzed MVP cleavage in human primary keratinocytes (HPKs) upon induction of apoptosis. UVB radiation as well as treatment with the kinase inhibitor staurosporine are inducers of apoptosis which is reflected by activation of the executioner caspase-3, the release of β-actin to the supernatant (Figure 4a and b) and of LDH (Supplementary Figure S2a). In addition, MVP was cleaved under these conditions. MVP cleavage and apoptosis were inhibited by treatment of HPKs with the pan-caspase inhibitor zVAD (Figure 4a and b), demonstrating that both processes depend on caspase activity. To test, whether MVP cleavage during cell death is a keratinocyte-specific event, we analyzed this process in human primary fibroblasts (HPFs). As these cells are very resistant to UVB radiation (Supplementary Figure S2b), we induced apoptosis with staurosporine and the chemotherapeutic drug mitoxantrone (Supplementary Figure S3 a and b). Comparable to the results obtained with HPKs (Figure 4a and b), MVP was cleaved in HPFs undergoing apoptosis and both processes were blocked by inhibition of caspase activity (Supplementary Figure S3 a and b). In contrast, MVP cleavage could not be detected in THP-1 cells undergoing cell death induced by different stimuli (Figure 4c and Supplementary Figure S2c). Thus, MVP is cleaved in a caspase-dependent manner in HPKs and HPFs during apoptosis, but not in THP-1 cells, where activation of GSDMD and pyroptosis occurs. Interestingly, cleavage of MVP in GSDMD-knockdown

HPKs in response to UVB irradiation occurs earlier and to a greater extent when compared to scrambled-transfected cells (Supplementary Figure S4).

In order to investigate whether in HPKs cleavage of endogenous MVP in response to UVB radiation and staurosporine requires caspase-1 and -9, we downregulated expression of the proteases by transfection of specific siRNAs (Supplementary Figure S10) and assessed MVP cleavage. We observed a decrease in MVP processing induced by different apoptotic stimuli in caspase-1 and -9 siRNA-silenced HPKs (Figure 4d) and in caspase-9 siRNA-silenced HPFs (Supplementary Figure S3c) compared to control cells (transfected with scrambled siRNA). Thus, both caspase-1 and caspase-9 are able to cleave MVP at the endogenous level in response to different cell death-inducing stimuli.

MVP cleavage by caspase-1/-9 causes its inactivation rather than its activation

GSDMD, proIL-1β and proIL-18 are well established caspase-1 substrates which gain activity upon processing by the protease. As MVP cleavage by caspase-1/-9 is associated with apoptosis and generates two fragments, p53 MVP NT and p54 MVP CT (Figure 2e), we tested whether their overexpression has any effects on cell death. We therefore transfected HEK293T cells (Supplementary Figure S5a) and HPKs (Supplementary Figure S5b) with plasmids encoding either full-length MVP, MVP NT, MVP CT or a combination of both fragments. Overexpression of neither of the cleavage products led to change in cell lysis when compared to transfection of cells with an empty vector. Then, we generated stably genetically modified HPFs allowing inducible overexpression of either MVP NT or MVP CT (Supplementary Figure S5c) and, after induction of gene expression, we triggered cell death by treatment with staurosporine. Neither overexpression of MVP NT nor MVP CT influenced cell lysis compared to control cells in response to this stimulus. These results suggest that MVP-derived fragments do not have a major role in cell death and that MVP is not activated upon cleavage.

MVP downregulation has been associated with reversal of multidrug resistance of cancer cells (Han et al., 2012, Herlevsen et al., 2007) and enhanced sensitivity to cell death (Pasillas et al., 2015, Ryu et al., 2008). Therefore, we analyzed the role of full-length MVP in HPKs in response to different apoptosis-inducing stimuli. We downregulated MVP expression in HPKs using two different specific siRNAs (Supplementary Figure S10) and induced cell death by UVB irradiation (Figure 5a) or treatment with staurosporine (Figure 5b). Cells with reduced MVP expression displayed increased cell death compared to control cells (cells transfected with scrambled siRNA), as reflected by the amount of β-actin in the supernatant and LDH release, cleaved caspase-3 positive and propidium iodide (PI) positive cells (Figure 5a and b). These effects were also observed in MVP-knockdown HPFs in response to treatment with staurosporine (Supplementary Figure S6a) or mitoxantrone (Supplementary Figure S6b). On the other hand, downregulation of MVP expression in HPKs did not influence IL-1β release nor GSDMD activation (p30) upon UVB irradiation (Supplementary Figure S7).

As caspase-1/-9 cleaved MVP in response to different apoptosis-inducing stimuli in epithelial cells and as its downregulation supported cell death, we hypothesized that this cleavage reflects a reduction in the total amount of full-length MVP. Indeed, the levels of full-length MVP were reduced in HPKs undergoing apoptosis upon UVB irradiation or staurosporine treatment (Figure 5c) and in HPFs treated with staurosporine or mitoxantrone (Supplementary Figure S6c). Furthermore, MVP mRNA levels were also reduced upon UVB-irradiation of HPKs (Supplementary Figure S8).

Taken together, these results confirm a role of MVP in cytoprotection. In addition, the caspase-1/-9-dependent processing of MVP causes reduction of the amount of the full-length protein. In turn, a decrease of the cellular level of full-length MVP might support cell death.

Cleavage-resistant MVP protects from cell death

In order to test, whether the specific cleavage of MVP at D441 is functionally relevant, we analyzed the consequences of overexpression of an MVP cleavage-resistant mutant in epithelial cells in the context of cell death. We generated HPKs (Figure 5d) and HPFs (Supplementary Figure S9) allowing inducible overexpression of either wt MVP, cleavage-resistant MVP(D441E) or eGFP. We induced overexpression of these proteins followed by induction of cell death by UVB irradiation (Figure 5d), treatment with staurosporine (Figure 5d and Supplementary Figure S9) or with mitoxantrone (Supplementary Figure S9). Overexpression of cleavage-resistant MVP(D441E) in HPKs and HPFs conferred protection against cell death (Figure 5d and Supplementary Figure S9). These experiments demonstrate that cleavage-resistant MVP is cytoprotective and, therefore, the functional relevance of the specific cleavage at D441.

DISCUSSION

Caspase-1 plays a central role in inflammation by activating and regulating the secretion or/and release of the proinflammatory cytokines proIL-1β and -18 (Dinarello, 2009). Furthermore, caspase-1 activity is required for unconventional secretion of at least some leaderless proteins in various cell types (Keller et al., 2008). Caspase-1 can induce a lytic type of cell death, termed pyroptosis, which is mainly described in immune cells and is induced by several different stimuli (Miao et al., 2011). This is caused by pore formation by the amino-terminal GSDMD fragment generated upon GSDMD activation by caspase-1 or other inflammatory caspases (Kayagaki et al., 2015, Shi et al., 2015). GSDMD-mediated pore formation allows release of IL-1β and -18 from pyroptotic cells.

UVB-irradiated HPKs secrete IL-1β/-18 after about 5 hours (Faustin and Reed, 2008, Feldmeyer et al., 2007, Fenini et al., 2018b). However, these cells do not undergo pyroptosis, but die by apoptosis several hours later (Sollberger et al., 2015). Our experiments demonstrate

that GSDMD, although expressed by HPKs, is only a poor caspase-1 substrate in HPKs in contrast to inflammasome-activated THP-1 cells. Instead, GSDMD is degraded in apoptotic HPKs, as reflected by appearance of a band for cleaved GSDMD with a different molecular weight than the active N-terminal p30 fragment. This different processing is most likely mediated by caspase-3 (Taabazuing et al., 2017). Interestingly, a knockdown of GSDMD expression revealed that the low levels of processed and active GSDMD in UVB-irradiated HPKs contributed to secretion of IL-1β, suggesting a role of GSDMD in the unconventional secretion pathway. A recent report demonstrated that caspase-1 initiates caspase-3-dependent apoptosis in GSDMD-deficient macrophages (Tsuchiya et al., 2019). Indeed, UVB-irradiated GSDMD-knockdown HPKs are characterized by more cleaved caspase-3 suggesting more apoptosis although the release of LDH was also reduced. These data suggest that inflammasome-induced GSDMD pores act like a valve for release/secretion of caspase-1 and other proapoptotic proteins (Keller et al., 2008), therefore withholding caspase-1-dependent apoptosis. 24 hours after UVB irradiation, apoptotic GSDMD-knockdown HPKs released similar amounts of IL-1β as control cells. This release might be mediated by caspase-3-induced activation of GSDME and formation of GSDME pores, as GSDME is activated by caspase-3 in HPKs (Wang et al., 2017). In conclusion, compared to inflammasome-activated immune cells, caspase-1 activates only low amounts of GSDMD in UVB-irradiated HPKs. This is not sufficient to induce pyroptosis at early time points in these cells. However, this activation supports unconventional secretion of IL-1β and prevents caspase-3 activation, which occurs only at late time points in UVB-irradiated HPKs.

UVB radiation is the most important risk factor for non-melanoma skin cancer (Leiter et al., 2014). UVB-induced apoptosis of keratinocytes is very relevant for skin cancer development, as cell death of damaged tumor cell precursors antagonizes cancer initiation. There is increasing evidence of a function of caspase-1 in apoptosis, including UVB-induced apoptosis of HPKs (Denes et al., 2012, Sollberger et al., 2015, Sun and Scott, 2016, Tsuchiya et al.,

2019). However, the downstream pathways and substrates of caspase-1 mediating these processes are poorly described. By a proteomics screen, we identified MVP as a substrate of caspase-1, cleaved at the D441 residue. In addition, caspase-9 is also able to cleave MVP in a similar manner as caspase-1. Caspase-9 is an established initiator apoptotic caspase (Kaufmann and Hengartner, 2001, Wurstle et al., 2012) and our results suggest a crosstalk with caspase-1 in the context of apoptosis, also confirmed by a recent publication (Tsuchiya et al., 2019). Indeed, both proteases contribute to apoptosis and MVP processing in HPKs. Our results confirm earlier reports of an involvement of caspase-9 in UVB-induced apoptosis (Sitailo et al., 2002, Takahashi et al., 2001) and support the concept of a role of caspase-1 in apoptosis, which is becoming increasingly evident (Denes et al., 2012, Sun and Scott, 2016, Tsuchiya et al., 2019).

MVP is a highly conserved protein and the main component of vaults, which are the biggest ribonucleoprotein particles of the cell (Berger et al., 2009). These organelles are believed to be involved in several processes, including cell death resistance (Herlevsen et al., 2007, Kowalski et al., 2007, Pasillas et al., 2015, Ryu et al., 2008, Scheffer et al., 2000, Teng et al., 2017). However, the exact molecular mechanisms, which underlie the role of MVP in cytoprotection are not known. Our experiments demonstrate a specific cleavage of MVP at the D441 residue by caspase-1 and -9 in apoptotic cells inducing a reduction in the amounts of full-length protein. MVP is a very stable protein with a half-life of 3 days (Zheng et al., 2005). Therefore, a rapid downregulation of the full-length form is only possible upon specific processing and our results suggest that caspase-1 and -9 are involved in this process by cleaving MVP at residue D441. Downregulation of MVP expression sensitizes cells to apoptosis and, most importantly, overexpression of cleavage-resistant MVP protects cells from cell death, demonstrating a functional role of the caspase-specific cleavage. Moreover, in GSDMD-knockdown UVB-irradiated HPKs, cleavage of MVP and caspase-3 occurs earlier than in control cells, further supporting that MVP processing is an event related to apoptosis.

Cleavage of MVP has never been described before. Our results demonstrate a crosstalk of MVP with caspase-1/-9 and a negative regulation of this cytoprotective protein by these caspases. As caspase-dependent inactivation of MVP occurs during apoptosis induced by several treatments in epithelial cells, this might represent a more general event occurring in apoptotic cells. However, more efforts are needed in order to elucidate the molecular mechanisms underlying the cytoprotective function of MVP.

MVP cleavage by caspase-1/-9 could be detected in HPKs and HPFs, but not in THP-1 cells. Instead, the levels of cleaved GSDMD upon caspase-1 activation were low in HPKs compared to pyroptotic THP-1 cells and pyroptosis could not be demonstrated in HPKs. This suggests a certain cell type-specificity for GSDMD-mediated pyroptosis. This event seems to be associated more with inflammasome-activated immune cells than with keratinocytes. Keratinocytes in the epidermis represent an indispensable barrier and pyroptosis might be incompatible with this essential function. However, how caspase-1 discriminates between MVP and GSDMD (and possibly other substrates) in these different cell types remains an open question. The factors, which regulate substrate specificity of the protease, are not fully elucidated. It has been suggested that posttranslational modifications or binding proteins of GSDMD determine how efficiently it is cleaved, activated or degraded (Aglietti and Dueber, 2017). This might be also the case for other caspase-1 substrates and even for the protease itself.

MATERIALS AND METHODS

Culture and treatment of primary cells

Isolation and culture of human primary keratinocytes (HPKs) was performed as described previously (Fenini et al., 2018a). HPKs were grown in serum-free keratinocyte medium (KSFM, Thermo Fisher Scientific, Waltham, US-MA) supplemented with epidermal growth factor (EGF) and bovine pituitary extract (BPE). Cells were harvested in trypsin/EDTA solution (0.05%/0.02% w/v) (Thermo Fisher Scientific) and cultured for at least 48 h before experiments. Cells were pre-treated with 10 μM pan-caspase inhibitor zVAD (Enzo Life Sciences, New York, US-NY) for 1 h before stimulation. HPKs were stimulated with either a dose of 1.75 J/cm^2 UVA, 0.0875 J/cm^2 of UVB (UV802L; Waldmann, Villingen-Schwenningen, Germany), 0.5 μM staurosporine (Sigma-Aldrich, St.Louis, US-MO), 3 μM talabostat (Selleckchem, Houston, US-TX) or transfected with ultra-pure LPS (upLPS, InvivoGen, San Diego, US-CA). Prior transfection with upLPS, cells were treated overnight with 20 ng/ml interferon γ (IFNγ, Peprotech, Rocky Hill, US-NJ). Transfection with 2 μg/ml upLPS was performed using Mirus TransIT-X2 (Mirus Bio LLC, Madison, US-WI) as transfection reagent. For siRNA-mediated knockdown, cells were transfected with 10 nM siRNAs (Sigma-Aldrich, Supplementary Table 1) using Interferin (Polyplus, Illkirch, France) as a transfection reagent.

Human primary fibroblasts (HPFs) were isolated from human dermis upon incubation with a solution of 1 mg/ml collagenase (Sigma-Aldrich) and 0.05 mM $CaCl_2$ in PBS for 2 h at 37 °C. A single cell suspension was obtained by passing the cells through a 100 μm cell strainer in DMEM (Thermo Fisher Scientific) containing 25% FBS (PAN-Biotech, Aidenbach, Germany) and 1% antibiotic/antimycotic (A/A, Thermo Fisher Scientific). HPFs were grown in DMEM supplemented with 10% FBS and 1% A/A, harvested in trypsin/EDTA solution (0.05%/0.02% w/v) and cultured for at least 48 h before experiments. Cells were pre-treated

with 10 μM pan-caspase inhibitor zVAD for 1 h before stimulation. For siRNA-mediated knockdown, cells were transfected as described above. HPFs were treated with either 0.5 μM staurosporine, the indicated dose of mitoxantrone (Sigma-Aldrich), exposed to a dose of 1.75 J/cm^2 UVA or 0.0875 J/cm^2 of UVB.

Human biopsies

The skin biopsies were collected with informed written consent upon approval from Local Ethical Committees and were conducted according to the Declaration of Helsinki Principles.

DATA AVAILABILITY

No datasets were generated or analyzed during the current study.

CONFLICTS OF INTEREST

The authors declare no competing interests.

ACKNOWLEDGEMENTS

We thank the Tagesklinik für Kinderchirurgie (Fällanden, Switzerland) for providing skin biopsies. This work was supported by grants from the Wilhelm-Sander Stiftung (Germany), the Promedica Stiftung (Switzerland), the Science Foundation for Oncology (Switzerland), the Georg und Bertha Schwyzer-Winiker-Stiftung (Switzerland), the Swiss Cancer Research (KFS-2741 and 3940), the Theodor und Ida Herzog-Egli-Stiftung (Switzerland), the Vontobel Stiftung (Switzerland) and the Novartis Foundation (Switzerland). SG, GF, PH and MDF were/are members of the Life Science Zurich Graduate School.

AUTHOR CONTRIBUTIONS

Concept: SG and HDB. Analysis: SG, GF, and TK. Funding: HDB. Investigation: SG, GF, TK, PH, and MDF. Resources: TK and HDB. Supervision: TK and HDB. Visualization: SG and GF. Original manuscript draft: SG and HDB. Manuscript review: GF and HDB.

REFERENCES

Aglietti RA, Dueber EC. Recent Insights into the Molecular Mechanisms Underlying Pyroptosis and Gasdermin Family Functions. Trends Immunol 2017;38(4):261-71.

Bell RAV, Megeney LA. Evolution of caspase-mediated cell death and differentiation: twins separated at birth. Cell death and differentiation 2017;24(8):1359-68.

Berger W, Steiner E, Grusch M, Elbling L, Micksche M. Vaults and the major vault protein: novel roles in signal pathway regulation and immunity. Cell Mol Life Sci 2009;66(1):43-61.

Broz P, Dixit VM. Inflammasomes: mechanism of assembly, regulation and signalling. Nature reviews Immunology 2016;16(7):407-20.

Denes A, Lopez-Castejon G, Brough D. Caspase-1: is IL-1 just the tip of the ICEberg? Cell Death Dis 2012;3:e338.

Dinarello CA. Immunological and inflammatory functions of the interleukin-1 family. Annual review of immunology 2009;27:519-50.

Ding J, Wang K, Liu W, She Y, Sun Q, Shi J, et al. Pore-forming activity and structural autoinhibition of the gasdermin family. Nature 2016;535(7610):111-6.

Faustin B, Reed JC. Sunburned skin activates inflammasomes. Trends Cell Biol 2008;18(1):4-8.

Feldmeyer L, Keller M, Niklaus G, Hohl D, Werner S, Beer HD. The inflammasome mediates UVB-induced activation and secretion of interleukin-1beta by keratinocytes. Current biology : CB 2007;17(13):1140-5.

Fenini G, Grossi S, Contassot E, Biedermann T, Reichmann E, French LE, et al. Genome Editing of Human Primary Keratinocytes by CRISPR/Cas9 Reveals an Essential Role of the NLRP1 Inflammasome in UVB Sensing. J Invest Dermatol 2018a;138(12):2644-52.

Fenini G, Grossi S, Contassot E, Biedermann T, Reichmann E, French LE, et al. Genome editing of human primary keratinocytes by CRISPR/Cas9 reveals an essential role of the NLRP1 inflammasome in UVB sensing. The Journal of investigative dermatology 2018b.

Fuchs E, Raghavan S. Getting under the skin of epidermal morphogenesis. Nat Rev Genet 2002;3(3):199-209.

Grandemange S, Sanchez E, Louis-Plence P, Tran Mau-Them F, Bessis D, Coubes C, et al. A new autoinflammatory and autoimmune syndrome associated with NLRP1 mutations: NAIAD (NLRP1-associated autoinflammation with arthritis and dyskeratosis). Ann Rheum Dis 2017;76(7):1191-8.

Han M, Lv Q, Tang XJ, Hu YL, Xu DH, Li FZ, et al. Overcoming drug resistance of MCF-7/ADR cells by altering intracellular distribution of doxorubicin via MVP knockdown with a novel siRNA polyamidoamine-hyaluronic acid complex. J Control Release 2012;163(2):136-44.

Herlevsen M, Oxford G, Owens CR, Conaway M, Theodorescu D. Depletion of major vault protein increases doxorubicin sensitivity and nuclear accumulation and disrupts its sequestration in lysosomes. Mol Cancer Ther 2007;6(6):1804-13.

Jin Y, Birlea SA, Fain PR, Spritz RA. Genetic variations in NALP1 are associated with generalized vitiligo in a Romanian population. The Journal of investigative dermatology 2007a;127(11):2558-62.

Jin Y, Mailloux CM, Gowan K, Riccardi SL, LaBerge G, Bennett DC, et al. NALP1 in vitiligo-associated multiple autoimmune disease. N Engl J Med 2007b;356(12):1216-25.

Kaufmann SH, Hengartner MO. Programmed cell death: alive and well in the new millennium. Trends Cell Biol 2001;11(12):526-34.

Kayagaki N, Stowe IB, Lee BL, O'Rourke K, Anderson K, Warming S, et al. Caspase-11 cleaves gasdermin D for non-canonical inflammasome signalling. Nature 2015;526(7575):666-71.

Kedersha NL, Miquel MC, Bittner D, Rome LH. Vaults. II. Ribonucleoprotein structures are highly conserved among higher and lower eukaryotes. J Cell Biol 1990;110(4):895-901.

Keller M, Ruegg A, Werner S, Beer HD. Active caspase-1 is a regulator of unconventional protein secretion. Cell 2008;132(5):818-31.

Kleifeld O, Doucet A, auf dem Keller U, Prudova A, Schilling O, Kainthan RK, et al. Isotopic labeling of terminal amines in complex samples identifies protein N-termini and protease cleavage products. Nat Biotechnol 2010;28(3):281-8.

Kleifeld O, Doucet A, Prudova A, auf dem Keller U, Gioia M, Kizhakkedathu JN, et al. Identifying and quantifying proteolytic events and the natural N terminome by terminal amine isotopic labeling of substrates. Nat Protoc 2011;6(10):1578-611.

Kowalski MP, Dubouix-Bourandy A, Bajmoczi M, Golan DE, Zaidi T, Coutinho-Sledge YS, et al. Host resistance to lung infection mediated by major vault protein in epithelial cells. Science 2007;317(5834):130-2.

Leiter U, Eigentler T, Garbe C. Epidemiology of skin cancer. Adv Exp Med Biol 2014;810:120-40.

Levandowski CB, Mailloux CM, Ferrara TM, Gowan K, Ben S, Jin Y, et al. NLRP1 haplotypes associated with vitiligo and autoimmunity increase interleukin-1beta processing via the NLRP1 inflammasome. Proceedings of the National Academy of Sciences of the United States of America 2013;110(8):2952-6.
Liu X, Zhang Z, Ruan J, Pan Y, Magupalli VG, Wu H, et al. Inflammasome-activated gasdermin D causes pyroptosis by forming membrane pores. Nature 2016;535(7610):153-8.
Miao EA, Rajan JV, Aderem A. Caspase-1-induced pyroptotic cell death. Immunological reviews 2011;243(1):206-14.
Nakajima YI, Kuranaga E. Caspase-dependent non-apoptotic processes in development. Cell death and differentiation 2017;24(8):1422-30.
Okondo MC, Johnson DC, Sridharan R, Go EB, Chui AJ, Wang MS, et al. DPP8 and DPP9 inhibition induces pro-caspase-1-dependent monocyte and macrophage pyroptosis. Nat Chem Biol 2017;13(1):46-53.
Okondo MC, Rao SD, Taabazuing CY, Chui AJ, Poplawski SE, Johnson DC, et al. Inhibition of Dpp8/9 Activates the Nlrp1b Inflammasome. Cell Chem Biol 2018;25(3):262-7 e5.
Pasillas MP, Shields S, Reilly R, Strnadel J, Behl C, Park R, et al. Proteomic analysis reveals a role for Bcl2-associated athanogene 3 and major vault protein in resistance to apoptosis in senescent cells by regulating ERK1/2 activation. Mol Cell Proteomics 2015;14(1):1-14.
Ryu SJ, An HJ, Oh YS, Choi HR, Ha MK, Park SC. On the role of major vault protein in the resistance of senescent human diploid fibroblasts to apoptosis. Cell death and differentiation 2008;15(11):1673-80.
Salucci S, Burattini S, Battistelli M, Baldassarri V, Maltarello MC, Falcieri E. Ultraviolet B (UVB) irradiation-induced apoptosis in various cell lineages in vitro. Int J Mol Sci 2012;14(1):532-46.
Sand J, Haertel E, Biedermann T, Contassot E, Reichmann E, French LE, et al. Expression of inflammasome proteins and inflammasome activation occurs in human, but not in murine keratinocytes. Cell Death Dis 2018;9(2):24.
Scheffer GL, Schroeijers AB, Izquierdo MA, Wiemer EA, Scheper RJ. Lung resistance-related protein/major vault protein and vaults in multidrug-resistant cancer. Curr Opin Oncol 2000;12(6):550-6.
Shi J, Zhao Y, Wang K, Shi X, Wang Y, Huang H, et al. Cleavage of GSDMD by inflammatory caspases determines pyroptotic cell death. Nature 2015;526(7575):660-5.
Shi J, Zhao Y, Wang Y, Gao W, Ding J, Li P, et al. Inflammatory caspases are innate immune receptors for intracellular LPS. Nature 2014;514(7521):187-92.
Sitailo LA, Tibudan SS, Denning MF. Activation of caspase-9 is required for UV-induced apoptosis of human keratinocytes. The Journal of biological chemistry 2002;277(22):19346-52.
Sollberger G, Strittmatter GE, Grossi S, Garstkiewicz M, Auf dem Keller U, French LE, et al. Caspase-1 activity is required for UVB-induced apoptosis of human keratinocytes. The Journal of investigative dermatology 2015;135(5):1395-404.
Steiner E, Holzmann K, Elbling L, Micksche M, Berger W. Cellular functions of vaults and their involvement in multidrug resistance. Curr Drug Targets 2006;7(8):923-34.
Strowig T, Henao-Mejia J, Elinav E, Flavell R. Inflammasomes in health and disease. Nature 2012;481(7381):278-86.
Sun Q, Scott MJ. Caspase-1 as a multifunctional inflammatory mediator: noncytokine maturation roles. J Leukoc Biol 2016;100(5):961-7.
Taabazuing CY, Okondo MC, Bachovchin DA. Pyroptosis and Apoptosis Pathways Engage in Bidirectional Crosstalk in Monocytes and Macrophages. Cell Chem Biol 2017;24(4):507-14 e4.
Takahashi H, Honma M, Ishida-Yamamoto A, Namikawa K, Miwa A, Okado H, et al. In vitro and in vivo transfer of bcl-2 gene into keratinocytes suppresses UVB-induced apoptosis. Photochem Photobiol 2001;74(4):579-86.
Teng Y, Ren Y, Hu X, Mu J, Samykutty A, Zhuang X, et al. MVP-mediated exosomal sorting of miR-193a promotes colon cancer progression. Nat Commun 2017;8:14448.
Tsuchiya K, Nakajima S, Hosojima S, Thi Nguyen D, Hattori T, Manh Le T, et al. Caspase-1 initiates apoptosis in the absence of gasdermin D. Nat Commun 2019;10(1):2091.
van Zon A, Mossink MH, Scheper RJ, Sonneveld P, Wiemer EA. The vault complex. Cell Mol Life Sci 2003;60(9):1828-37.
Wang Y, Gao W, Shi X, Ding J, Liu W, He H, et al. Chemotherapy drugs induce pyroptosis through caspase-3 cleavage of a gasdermin. Nature 2017;547(7661):99-103.
Wurstle ML, Laussmann MA, Rehm M. The central role of initiator caspase-9 in apoptosis signal transduction and the regulation of its activation and activity on the apoptosome. Exp Cell Res 2012;318(11):1213-20.
Zheng CL, Sumizawa T, Che XF, Tsuyama S, Furukawa T, Haraguchi M, et al. Characterization of MVP and VPARP assembly into vault ribonucleoprotein complexes. Biochem Biophys Res Commun 2005;326(1):100-7.

Zhong FL, Mamai O, Sborgi L, Boussofara L, Hopkins R, Robinson K, et al. Germline NLRP1 Mutations Cause Skin Inflammatory and Cancer Susceptibility Syndromes via Inflammasome Activation. Cell 2016;167(1):187-202 e17.

FIGURE LEGENDS

Figure 1. Gasdermin D is not efficiently activated by caspase-1 in human primary keratinocytes (HPKs).

(**a**, left panel) Immunoblot analysis of human primary keratinocytes (HPKs) either UVB-irradiated (0.0875 J/cm^2), treated with staurosporine (0.5 µM), with talabostat (3 µM), transfected with upLPS (2 µg/ml), or left untreated and harvested after 5 h or 24 h as indicated. (**b**, left panel) Immunoblot analysis of stably genetically modified HPKs (Fenini et al., 2018a) either untreated or treated 20 h with doxycycline (1 µg/ml) to induce expression of eGFP or caspase-1 (wt)-FLAG. Untransduced keratinocytes (-) served as control. (**a** and **b**, right panels) Immunoblot analysis of HPKs (treated as described in **a** and **b,** left panels), side by side with differentiated and primed (upLPS 0.1 µg/ml, 16 h) THP-1 cells treated with nigericin (5 µM) for 2.5 h, after pre-treatment with either DMSO (-zVAD) or zVAD (10 µM) for 1 h. (**c**) Immunoblot analysis (left panel), analyses of LDH release (upper right panel) and of IL-1β release in the supernatant by ELISA (lower right panel) of HPKs 48 h after transfection with scrambled siRNA (ctr.) or GSDMD targeting siRNAs (GSDMD #1 and GSDMD #2) subjected to UVB irradiation (0.0875 J/cm^2) for 6 and 24 h or without treatment. Graph bars represent mean ± SEM of n = 4 independent experiments with HPKs from different donors with one-way ANOVA with Dunnet's multiple-comparison test (*$p<0.05$, **$p<0.01$). One representative Western blot from three experiments is shown.

Figure 2. Caspase-1 cleaves major vault protein (MVP) after D441 in human keratinocytes.

(**a**) 10-plex TMT-labelling scheme for TAILS shotgun proteomics analysis of genetically modified human primary keratinocytes (HPKs) treated with 1 µg/ml doxycycline for 20 h to

induce expression of the indicated proteins: eGFP, caspase-1 (wt)-FLAG and caspase-1 (mut)-FLAG. Peptides were identified by MS/MS and quantified by SPS-MS/MS/MS. (**b**) MS/MS spectrum of TAKSLQPLAPR, the neo-N-terminal peptide of the cleavage product of MVP identified by TAILS. (**c**) Peptide abundance (normalized), peptide abundance (grouped) and peptide abundance ratio (log2)/eGFP of the peptide corresponding to cleaved MVP identified by TMT-TAILS in the lysate of HPKs overexpressing eGFP, caspase-1 (wt)-FLAG and caspase-1 (mut)-FLAG. Graph bars represent mean ± SD of n = 3 biological replicates with one-way ANOVA with Dunnet's multiple-comparison test (****$p<0.0001$). (**d**) Caspase cleavage site (D441) in the MVP protein identified by TMT-TAILS. *Represents TMT-labelled residues. (**e**) Confirmation of MVP cleavage by immunoblotting of lysates of HPKs overexpressing eGFP, caspase-1 (wt)-FLAG and caspase-1 (mut)-FLAG using antibodies targeting either MVP N-term (NT) or MVP C-term (CT).

Figure 3. MVP is cleaved by caspase-1 and caspase-9 after D441.

(**a**) Coomassie blue stained SDS-polyacrylamide gels (above) and immunoblot analysis (below) of recombinant amino-terminal GST-tagged MVP (GST-MVP) incubated without (-) or with active p20/p10 tetramers of the indicated recombinant caspases (rCASPs). (**b**) Immunoblot analysis of HEK293T cells 24 h after transfection with plasmids encoding MVP in combination with either an empty vector (-) or plasmids encoding wild-type caspase-1 (wt) or wild-type FLAG-caspase-9 (wt). (**c**) Immunoblot analysis of HEK293T cells 24 h after transfection with plasmids encoding MVP and proIL-1β, in combination with either an empty vector (-) or plasmids encoding wild-type caspase-1 (wt), caspase-1 inactive mutant C285A (mut), wild-type caspase-4 (wt)-myc, caspase-4 inactive mutant C258A (mut) -myc or wild-type caspase-5 (wt) -myc. (**d**) Immunoblot analysis of HEK293T cells 24 h after transfection with either an empty vector (-) or a plasmid encoding wild-type caspase-1 (wt), in

combination with either an empty vector (-) or plasmids encoding wild-type MVP (MVP) or MVP mutants (D441A or D441E). Experiments were performed at least twice.

Abbreviations: GST-MVP NT: GST-tagged amino-terminal fragment of MVP; MVP CT: carboxy-terminal fragment of MVP; CT: targeting the carboxy-terminal part; NT: targeting the amino-terminal part.

Figure 4. MVP is cleaved by caspase-1/-9 in human primary keratinocytes (HPKs) but not in THP-1 cells.

(**a** and **b**) Immunoblot analysis (above) and quantification of the band corresponding to the cleaved MVP fragment (p54) normalized to β-actin (below) of HPKs either untreated, UVB-irradiated (0.0875 J/cm^2) (**a**) or treated with staurosporine (0.5 μM) (**b**) for 20 h, after pre-treatment with DMSO (-) or zVAD (10 μM) for 1 h. Graph bars in (**a** and **b**) represent mean ± SD of n = 3 independent experiments. (**c**) Immunoblot analysis of differentiated and primed (upLPS 0.1 μg/ml, 16 h) THP-1 cells stimulated with either nigericin (5 μM), UVB (0.0875 J/cm^2), staurosporine (0.5 μM) or left untreated (-), and harvested at the indicated time points. (**d**) Immunoblot analysis (above) and quantification of the band corresponding to the cleaved MVP fragment (p54) normalized to β-actin (below) of HPKs 48 h after transfection with scrambled siRNA (ctr.) or caspase-1 and caspase-9 targeting siRNAs, with either no treatment, UVB irradiation (0.0875 J/cm^2) or treatment with staurosporine (0.5 μM) for 20 h. Graph bars represent mean ± SD of n = 4 independent experiments with one-way ANOVA with Dunnet's multiple-comparison test (*$p<0.05$). One representative Western blot from three experiments is shown.

Abbreviations: CT: targeting the carboxy-terminal part.

Figure 5. MVP is a cytoprotective protein in human primary keratinocytes (HPKs).

(**a** and **b**) Immunoblot analysis (above left), analysis of LDH release (above right), FACS analysis of cleaved caspase-3 positive (%; below left) and PI positive cells (%; below right) of HPKs 48 h after transfection with scrambled siRNA (ctr.) or MVP targeting siRNAs (MVP #1 and MVP #2) subjected either to UVB irradiation (0.0875 J/cm^2) (**a**) or treatment with staurosporine (0.5 μM) (**b**) for 20 h. Graph bars in (**a** and **b**) represent mean ± SEM of n = 3 independent experiments with one-way ANOVA with Dunnet's multiple-comparison test (*p<0.05, **p<0.01). (**c**) Immunoblot analysis (above) of HPKs either untreated, UVB-irradiated (0.0875 J/cm^2) or treated with staurosporine (0.5 μM) for 20 h and quantification of the band corresponding to full-length MVP normalized to β-actin and relative to untreated cells (below). Error bars represent mean ± SD of n = 3 independent experiments with one-way ANOVA with Dunnet's multiple-comparison test (**=p<0.01). (**d**) Immunoblot analysis (left) and analysis of LDH release (right) of stably genetically modified HPKs treated 20 h with doxycycline (1 μg/ml) to induce expression of eGFP, MVP or MVP (D441E) and subjected either to UVB irradiation (0.0875 J/cm^2), treatment with staurosporine (0.5 μM) for 20 h or left untreated. Graph bars represent mean ± SEM of n = 3 independent experiments with two-way ANOVA with Turkey's multiple-comparison test (*=p<0.05). One representative Western blot from three experiments is shown.

Abbreviations: NT: targeting the amino-terminal part; CT: targeting the carboxy-terminal part; ns: not significant.

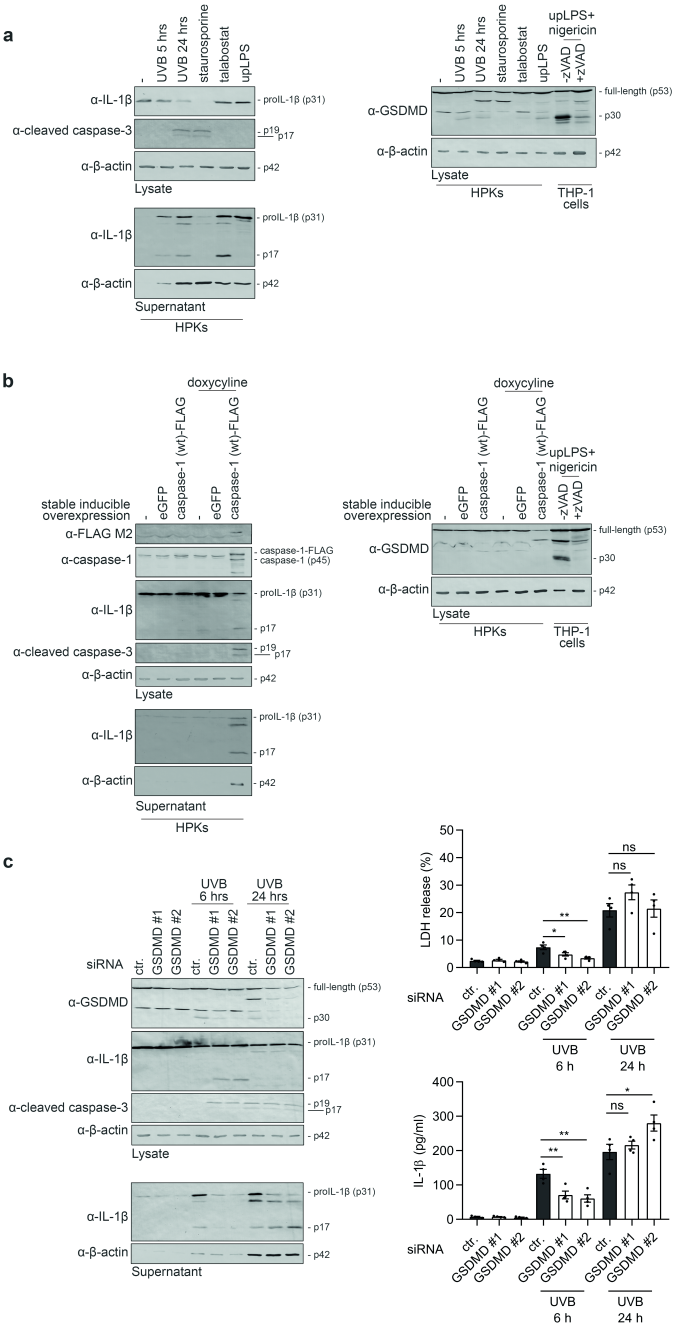

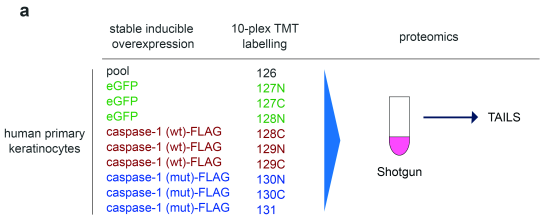
a
stable inducible overexpression
10-plex TMT labelling
proteomics
human primary keratinocytes
pool 126
eGFP 127N
eGFP 127C
eGFP 128N
caspase-1 (wt)-FLAG 128C
caspase-1 (wt)-FLAG 129N
caspase-1 (wt)-FLAG 129C
caspase-1 (mut)-FLAG 130N
caspase-1 (mut)-FLAG 130C
caspase-1 (mut)-FLAG 131
Shotgun
TAILS

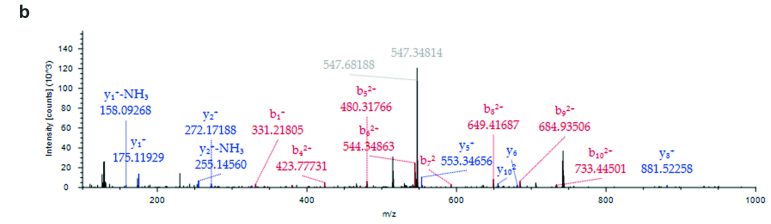
b
Intensity [counts] (10^3)
m/z
547.34814
547.68188
y1*-NH3 158.09268
y1* 175.11929
y2* 272.17188
y2*-NH3 255.14560
b1* 331.21805
b4++ 423.77731
b3++ 480.31766
b2++ 544.34863
b2 553.34656
y5* 649.41687
y6 y10++
b5++ 684.93506
b10++ 733.44501
y8* 881.52258

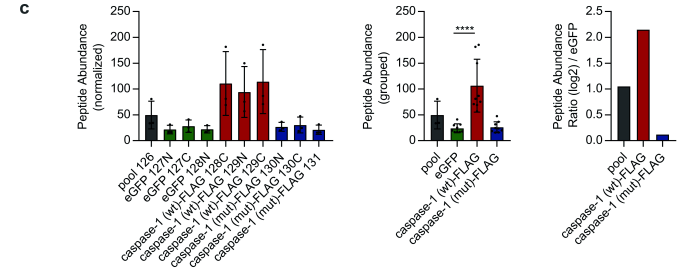
c
Peptide Abundance (normalized)
pool 126
eGFP 127N
eGFP 127C
eGFP 128N
caspase-1 (wt)-FLAG 128C
caspase-1 (wt)-FLAG 129N
caspase-1 (wt)-FLAG 129C
caspase-1 (mut)-FLAG 130N
caspase-1 (mut)-FLAG 130C
caspase-1 (mut)-FLAG 131
Peptide Abundance (grouped)
****
pool
eGFP
caspase-1 (wt)-FLAG
caspase-1 (mut)-FLAG
Peptide Abundance Ratio (log2) / eGFP

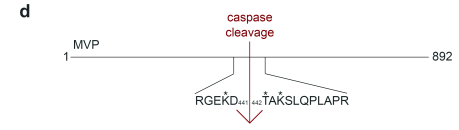
d
MVP
1
892
caspase cleavage
RGEKD441 442TAKSLQPLAPR

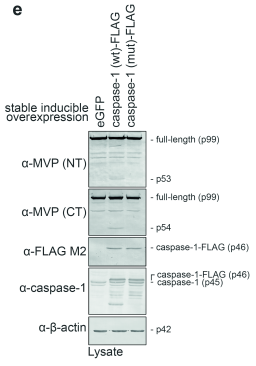
e
stable inducible overexpression
eGFP
caspase-1 (wt)-FLAG
caspase-1 (mut)-FLAG
α-MVP (NT)
full-length (p99)
p53
α-MVP (CT)
full-length (p99)
p54
α-FLAG M2
caspase-1-FLAG (p46)
α-caspase-1
caspase-1-FLAG (p46)
caspase-1 (p45)
α-β-actin
p42
Lysate

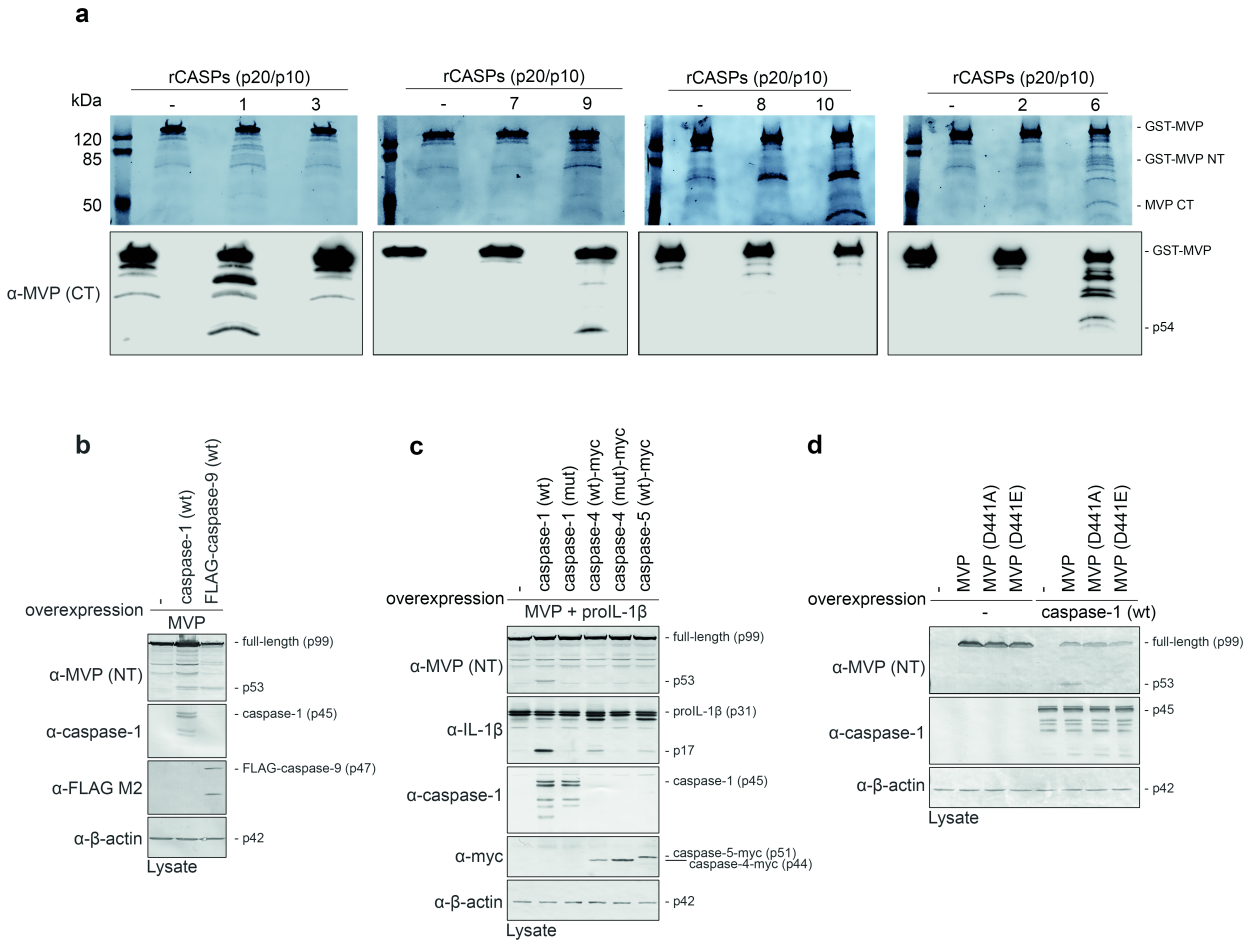
a
rCASPs (p20/p10)
kDa
-
1
3
7
9
8
10
2
6
120
85
50
- GST-MVP
- GST-MVP NT
- MVP CT
α-MVP (CT)
- GST-MVP
- p54
b
overexpression
-
caspase-1 (wt)
FLAG-caspase-9 (wt)
MVP
α-MVP (NT)
- full-length (p99)
- p53
α-caspase-1
- caspase-1 (p45)
α-FLAG M2
- FLAG-caspase-9 (p47)
α-β-actin
- p42
Lysate
c
caspase-1 (wt)
caspase-1 (mut)
caspase-4 (wt)-myc
caspase-4 (mut)-myc
caspase-5 (wt)-myc
MVP + proIL-1β
α-IL-1β
- proIL-1β (p31)
- p17
α-myc
- caspase-5-myc (p51)
caspase-4-myc (p44)
d
MVP
MVP (D441A)
MVP (D441E)
caspase-1 (wt)
- p45

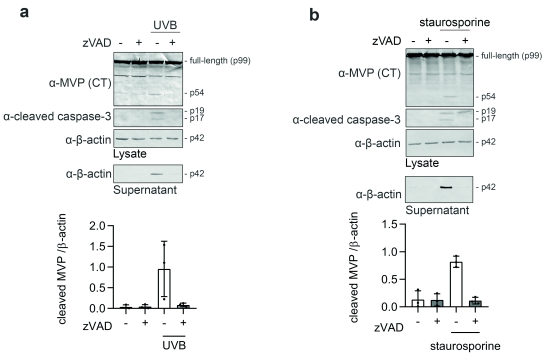
a
UVB
zVAD - + - +
full-length (p99)
α-MVP (CT)
p54
α-cleaved caspase-3
p19
p17
α-β-actin
p42
Lysate
α-β-actin
p42
Supernatant
cleaved MVP /β-actin
2.0
1.5
1.0
0.5
0.0
zVAD - + - +
UVB
b
staurosporine
zVAD - + - +
full-length (p99)
α-MVP (CT)
p54
α-cleaved caspase-3
p19
p17
α-β-actin
p42
Lysate
α-β-actin
p42
Supernatant
cleaved MVP /β-actin
1.5
1.0
0.5
0.0
zVAD - + - +
staurosporine

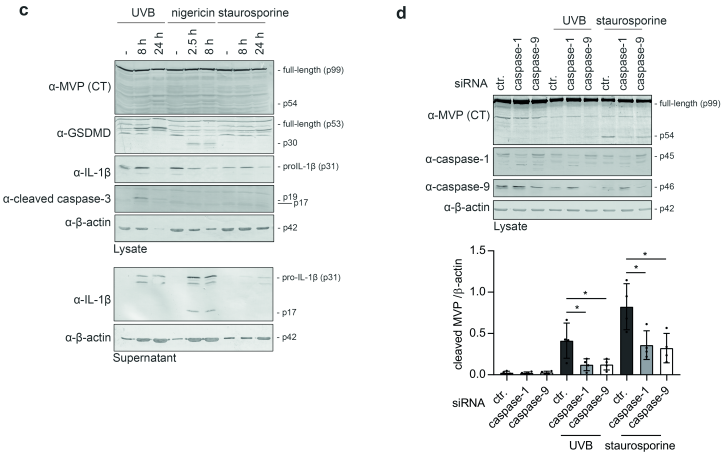
c
UVB nigericin staurosporine
- 8 h 24 h - 2.5 h 8 h - 8 h 24 h
full-length (p99)
α-MVP (CT)
p54
full-length (p53)
α-GSDMD
p30
proIL-1β (p31)
α-IL-1β
α-cleaved caspase-3
p19
p17
α-β-actin
p42
Lysate
pro-IL-1β (p31)
α-IL-1β
p17
α-β-actin
p42
Supernatant
d
UVB staurosporine
siRNA ctr. caspase-1 caspase-9 ctr. caspase-1 caspase-9 ctr. caspase-1 caspase-9
full-length (p99)
α-MVP (CT)
p54
p45
α-caspase-1
p46
α-caspase-9
α-β-actin
p42
Lysate
cleaved MVP /β-actin
1.5
1.0
0.5
0.0
siRNA ctr. caspase-1 caspase-9 ctr. caspase-1 caspase-9 ctr. caspase-1 caspase-9
UVB staurosporine

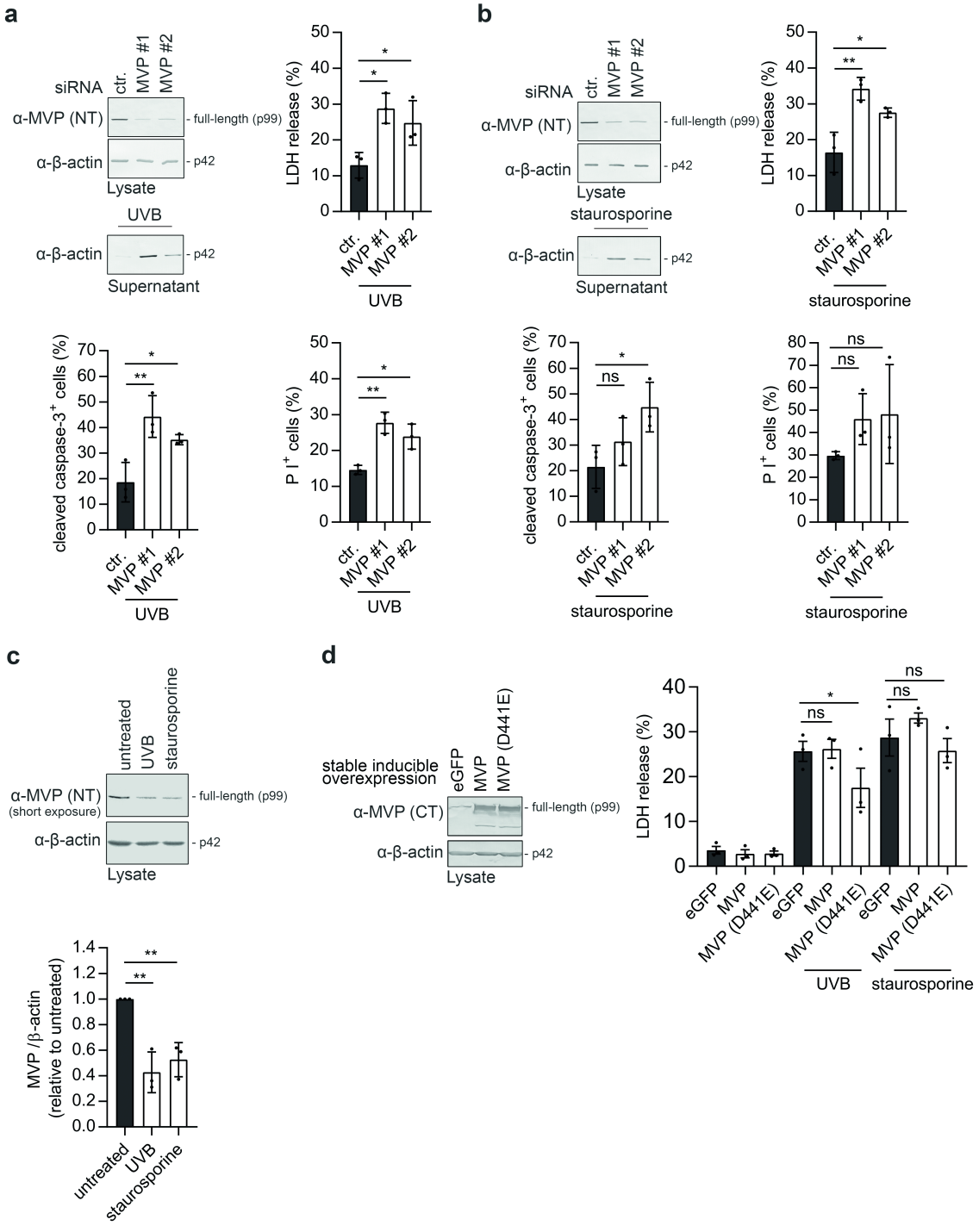
a
siRNA
ctr.
MVP #1
MVP #2
α-MVP (NT)
- full-length (p99)
α-β-actin
- p42
Lysate
UVB
α-β-actin
- p42
Supernatant
LDH release (%)
ctr.
MVP #1
MVP #2
UVB
cleaved caspase-3+ cells (%)
PI+ cells (%)
b
staurosporine
ns
c
untreated
UVB
staurosporine
α-MVP (NT)
(short exposure)
MVP /β-actin
(relative to untreated)
d
stable inducible
overexpression
eGFP
MVP
MVP (D441E)
α-MVP (CT)

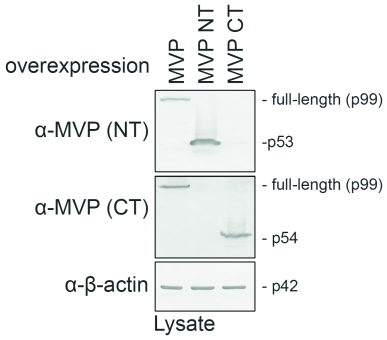

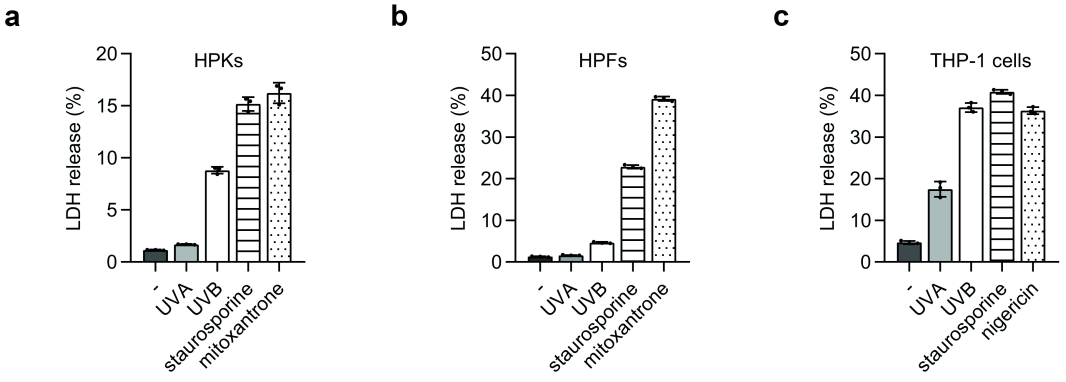

SUPPLEMENTARY MATERIAL

Supplementary Methods

Culture and treatment of cell lines

HEK293T cells (ATCC CRL-3216, Manassas, US-VA) were cultured in DMEM supplemented with 10% FBS and 1% A/A and harvested with trypsin/EDTA solution (0.05%/0.02% w/v).

THP-1 cells (ATCC TIB-202) were cultured in RPMI 1640 (Thermo Fisher Scientific) supplemented with 10% FBS, 1% A/A, 1 mM Sodyum Pyruvate (Thermo Fisher Scientific) and 1% GlutaMax (Thermo Fisher Scientific). Before experiments, cells were differentiated with 15 ng/ml phorbol 12-myristate 13-acetate (PMA) (Sigma-Aldrich) for 3 days and primed with 0.1 μg/ml upLPS for 16 h. One h before experiments, the medium was replaced by Opti-MEM (Thermo Fisher Scientific) and cells were exposed to a dose of 1.75 J/cm^2 UVA, 0.0875 J/cm^2 UVB, treated with 0.5 μM staurosporine or with 5 μM nigericin (Selleckchem). All cells were grown at 37 °C in 5% CO_2 and 95% humidity.

Manipulation of cells

Plasmid transfection of HEK293T cells and HPKs for overexpression was performed in Opti-MEM (Thermo Fisher Scientific) and KSFM respectively using the TransIT-X2 (Mirus Bio LLC) transfection system according to manufacturer's instructions. Cell lysate and supernatant were harvested 24 h after transfection.

Stably genetically modified human primary keratinocytes (HPKs) and fibroblasts (HPFs) were generated by transduction of cells with lentiviruses encoding for the gene of interest under the control of an inducible promoter (pLenti CMVtight Puro DEST; Addgene, #26430) and lentiviruses encoding the reverse tetracycline-controlled transactivator 3 (rtTA3) (pLenti CMV rtTA3 Blast; Addgene, #26429). Lentiviruses were produced as described previously (Fenini et al., 2018). After transduction, cells were selected with 2.5 μg/ml puromycin

(Sigma-Aldrich) and 2.5 µg/ml blasticidin (Sigma-Aldrich). Transduction and selection of HPKs was performed in co-culture with antibiotics-resistant 3T3-J2 feeder cells as described previously (Fenini et al., 2018). Overexpression of the protein of interest was induced upon overnight (20 h) treatment of cells with 1 µg/ml doxycycline (Sigma-Aldrich).

In vitro MVP cleavage by recombinant caspases

For cleavage by the p20/p10 tetramers of active caspase, 3.5 µg of recombinant amino-terminal GST-tagged MVP (Abnova H00009961-P01, Taiwan) were incubated with 1 unit of caspase-1, -3, -7, -9, -8, -10, -2 and -6 in a 35 µl reaction containing 50 mM HEPES (pH 7.5), 3 mM EDTA, 150 mM NaCl, 0.005% (v/v) Tween-20 and 10 mM DTT. The reaction was incubated for 5 h at 37 °C. Reaction samples were separated on SDS-PAGE gels and cleavage of MVP was examined by Coomassie Brilliant Blue staining (Thermo Fisher Scientific) and immunoblotting.

Immunoblotting

Cell culture supernatants were precipitated by adding 2.5 volumes of acetone (100% w/v, Sigma-Aldrich), overnight incubation at -20°C and centrifugation for 2 h (4000 x g, 4°C). Proteins were separated by SDS-PAGE and analyzed by immunoblotting as previously described (Fenini et al., 2018). The primary antibodies used are anti-β-actin (A5441) and anti-FLAG M2 (F1804) from Sigma-Aldrich, anti-cleaved caspase-3 (#9661L) from Cell Signaling Technology (Danvers, US-MA), anti-caspase-1 (sc622) and anti-caspase-9 (sc133109) from Santa Cruz Biotechnology (Santa Cruz, US-CA), anti-IL-1β (MAB201) from R&D Systems (Minneapolis, US-MN), anti-myc (#631206) from Clontech Laboratories (Mountain View, US-CA), anti-MVP (NT) (ab14562) and anti-MVP (CT) (ab175239) from Abcam (Cambridge, UK), and anti-gasdermin D (NBP2-33422) from Novus Biologicals (Centennial, US-CO).

Analysis of cell death

Cell lysis was assessed by measuring the release of lactate dehydrogenase (LDH) in the supernatants by using the CytoTox 96 non-radioactive cytotoxicity assay (Promega, Fitchburg, US-WI) according to manufacturer's instructions. Results are shown as percentage LDH release (LDH in the supernatant/total LDH × 100).

For flow cytometry analysis, adherent cells were collected upon incubation with accutase (GE Healthcare Bio-Sciences, Pasching, Austria) and stained with 0.05 mg/ml propidium iodide (PI). Alternatively, collected cells were fixed with 2% paraformaldehyde (PFA) (Sigma-Aldrich), permeabilized with saponin, and incubated with anti-cleaved caspase-3 (#39661L) primary antibody followed by APC-conjugated anti-rabbit IgG (#711-136-152; Jackson, West Grove, US-PA) secondary antibody at room temperature for 45 minutes each.

ELISA

Release of human IL-1β in the supernatant was measured by ELISA (R&D Systems) according to manufacturer's instructions. Corresponding cell lysates were lysed for 30 minutes in 10% Triton X-100, centrifuged and supernatants used for the assay.

TMT-TAILS

TMT-TAILS was performed as described by (Kockmann et al., 2016) with minor changes. Briefly, 100 µg of each protein sample diluted in TAILS buffer (2.5 M GnHCl, 250 mM HEPES pH 7.8) were denaturated, reduced and alkylated. TMT10plex Isobaric Labels (Thermo Fisher Scientific) diluted in DMSO were transferred to the corresponding sample, incubated for 1 h at room temperature and reactions were subsequently quenched with 1 M ammonium bicarbonate solution. TMT-labeled samples were combined, and proteins were precipitated with 8 volumes of ice-cold acetone and 1 volume of ice-cold methanol for 2 h at -

80 °C. Protein pellet was obtained by centrifugation, washed with ice-cold methanol and the precipitate collected again by centrifugation. The protein pellet was dried and resuspended in 0.1 M NaOH solution. The dissolved proteins were diluted in ddH_2O and HEPES (pH 7.8). Labeled proteins were digested with Sequencing Grade Modified Trypsin (Promega) (ratio trypsin to total protein 1:50 w/w) overnight at 37 °C. The pH of the peptide solution was adjusted to 6.5-7 and the samples were incubated with HPG-ALD polymer (obtained from: Flintbox Innovation Network, (http://www.flintbox.com/public/project/1948)) and sodium borohydride solution (Sigma-Aldrich) overnight at 37 °C with gentle shaking. The free unbound peptides were filtered with a 30 kDa Amicon filter (Millipore, Billerica, US-MA) and the filtrate collected and subjected to C18 peptide cleanup using Finisterre C18 SPE Columns (Teknokroma, Barcelona, Spain).

Peptides were dried, dissolved in LC-MS solution (3% acetonitrile, 0.1% formic acid) and analyzed by LC-MS/MS using a nano-flow UHPLC system (EASY-Nlc 1200 System, Thermo Fisher Scientific) coupled to an Orbitrap Fusion Tribid mass spectrometer (Thermo Fisher Scientific). Peptides were eluted by gradually increasing acetonitrile from 0 to 37% in 60 min (flow rate 250 nl/min), ions accumulated to a target value of 5×10^5, and full scan MS acquired with a resolution of 60000 at 350-1250 m/z scan range. The 15 most intense signals above a threshold of 1000 were subjected to collision-induced dissociation (CID) to record MS/MS spectra in a data-dependent manner in the ion trap using a normalized collision energy of 35% and an activation time of 10 ms. To record TMT report ions, the same precursors were fragmented using higher collisional dissociation (HCD) with a normalized collision energy of 35% recording spectra at a resolution of 60000 at 100 m/z. Single charge states were rejected, charge state screening enabled and an exclusion window of 20 ppm applied. Precursor masses already selected for MS/MS were excluded for further selection for 45 s.

Peak lists were extracted from raw files and corresponding CID/HCD spectra pairs merged using Proteome Discoverer v2.1 (Thermo Fisher Scientific). Proteome Discoverer v2.1 was used to search peak lists (mgf) against human UniProtKB database (taxonomy 9606; release 2016_6; 71579 entries), to which reversed decoy sequences as well as sequences from common contaminants had been added. Searches were performed setting Trypsin-R (semi) for enzyme specificity (0 missed cleavage), carbamidomethyl(C) as fixed modification, TMT(K), TMT(N-term) and oxidation(M) as dynamic modifications for the peptides, and acetyl(N-term), Met-loss(N-term) and Met-loss+Acetyl(N-term) as dynamic modifications for proteins. Parent mass error and fragment mass error were set at 10 ppm and 0.8 Da respectively. Differentially abundant N-termini (TAILS) were determined for all channels using Proteome Discoverer 2.1 by extracting only N-terminally labelled peptides or naturally blocked semitryptic peptides. Then, the union of peptides from all experiments was formed and intensity weighted abundance ratios were calculated from all spectra per peptide. The experimental variation was derived from the ratio distribution of natural N-termini. Log2 ratios of abundances (log2(caspase-1 wt/eGFP) and log2(caspase-1 mut/eGFP)) were calculated and peptides with log2 ratios of > 1.2 or < -1.2 were considered to be significantly increased or decreased in abundance respectively compared to the eGFP control.

Real-time PCR

Levels of caspase-1, caspase-9, GSDMD and MVP mRNA were determinded by quantitative real-time PCR using a LightCycler 480 instrument (Roche, Rotkreuz, Switzerland) and LightCycler 480 SYBR Green Master (Roche). mRNA levels were normalized to RPL27. Primers were purchased from Microsynth (Balgach, Switzerland) (Supplementary Table 2).

Statistical analysis

All data were statistically analyzed using GraphPad Prism 7.02 software (GraphPad Software, Inc., La Jolla, US-CA). Comparison of three or more groups was performed using either one-way or two-way ANOVA, with Dunnett's correction if all groups were compared to one control group, or with Tukey's correction, if several groups were compared to other groups. Differences were considered significant when P-values were below 0 (****$p<0.0001$, **$p<0.01$, *$p<0.05$). All data are displayed as mean ± standard error of mean (SEM) of three independent experiments, unless otherwise stated.

Supplementary Tables

Target	Gene Symbol	Sense siRNA sequence	Antisense siRNA sequence
control (ctr.)	-	(UUCUCCGAACGUGUCACGU)(dT)(dT)	(dA)(dA)(ACGUGACACGUUCGGAGAA)
caspase-1	CASP1	(AAGAGAUCCUUCUGUAAAGGU)(dT)(dT)	(dA)(dA)(ACCUUUACAGAAGGAUCUCUU)
caspase-9	CASP9	(CGCUAAUGCUGUUUCGGUG)(dT)(dT)	(dA)(dA)(GCGAUUACGACAAAGCCAC)
MVP #1	MVP	(CGAGAAAGCUCGCAAGGAA)(dT)(dT)	(dA)(dA)(UUCCUUGCGAGCUUUCUCG)
MVP #2	MVP	(CUGUGAUUGGAAGCACCUA)(dT)(dT)	(dA)(dA)(UAGGUGCUUCCAAUCACAG)
GSDMD #1	GSDMD	CUCUGACUUGGACGUCCUU(dT)(dT)	(dA)(dA)(CUCUGACUUGGACGUCCUU)
GSDMD #2	GSDMD	GUGUCAACCUGUCUAUCAA(dT)(dT)	(dA)(dA)(CACAGUUGGACAGAUAGUU)

Supplementary Table S1.

Sense and antisense sequences of the siRNAs used in Fig. 1, 4, 5 and Supplementary Fig. 3, 4, 6 and 7.

Genes	Forward primer	Reverse primer
Human caspase-1	5`- AGTGCAGGACAACCCAGCTA -3`	5`- AGATAATGAGAGCAAGACGTGTG -3’
Human caspase-9	5`- CTTCGTTTCTGCGAACTAACAGG -3’	5`- GCACCACTGGGGTAAGGTTT -3’
Human GSDMD	5`- GTGTGTCAACCTGTCTATCAAGG -3’	5`- CATGGCATCGTAGAAGTGGAAG -3’
Human MVP	5’- TACATCCGGCAGGACAATGAG -3’	5’- CTGTGCAGTAGTGACGTGGG -3’
Human RPL27	5’- ATCGCCAAGAGATCAAAGATAA -3’	5’- TCTGAAGACATCCTTATTGACG -3’

Supplementary Table S2.

List of real-time PCR primers used in Supplementary Fig. 8 and 10.

Supplementary Figures

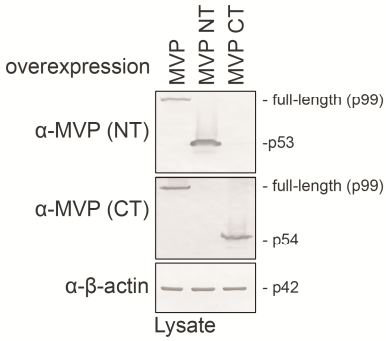

Supplementary Figure S1. MVP antibodies specificity.

Immunoblot analysis of HEK293T cells 24 h after transfection with plasmids encoding either wild-type MVP (MVP), the amino-terminal fragment of MVP (MVP NT) or the carboxy-terminal fragment (MVP CT) of MVP.

Abbreviations: NT: targeting the amino-terminal part; CT: targeting the carboxy-terminal part.

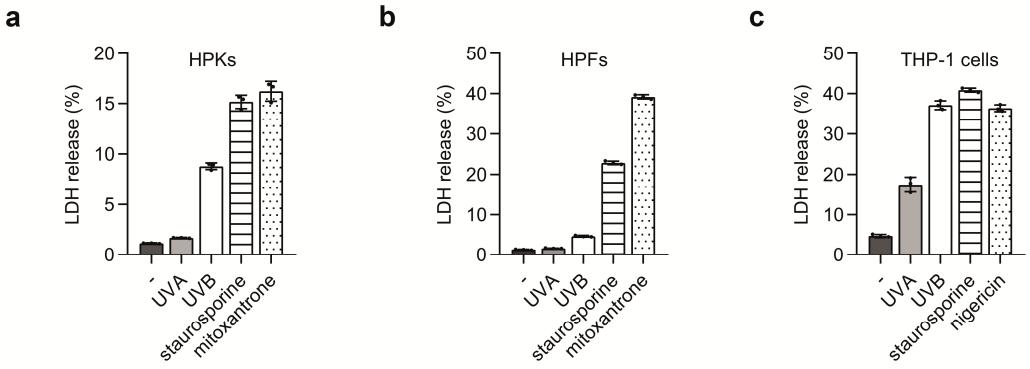

Supplementary Figure S2. Response of human primary keratinocytes (HPKs), fibroblasts (HPFs) and THP-1 cells to different cell death-inducing stimuli.

Analysis of LDH release (**a** - **c**) of HPKs (**a**), HPFs (**b**) and of differentiated and upLPS-primed (0.1 μg/ml, 16 h) THP-1 cells (**c**) left untreated (-) or treated as indicated: UVA (1.75 J/cm^2, 20 h), UVB (0.0875 J/cm^2, 20 h), staurosporine (0.5 μM, 20 h), mitoxantrone (25 μM, 20 h) and nigericin (5 μM, 2.5 h). Graph bars represent mean ± SD of technical replicates from a single experiment (n = 1).

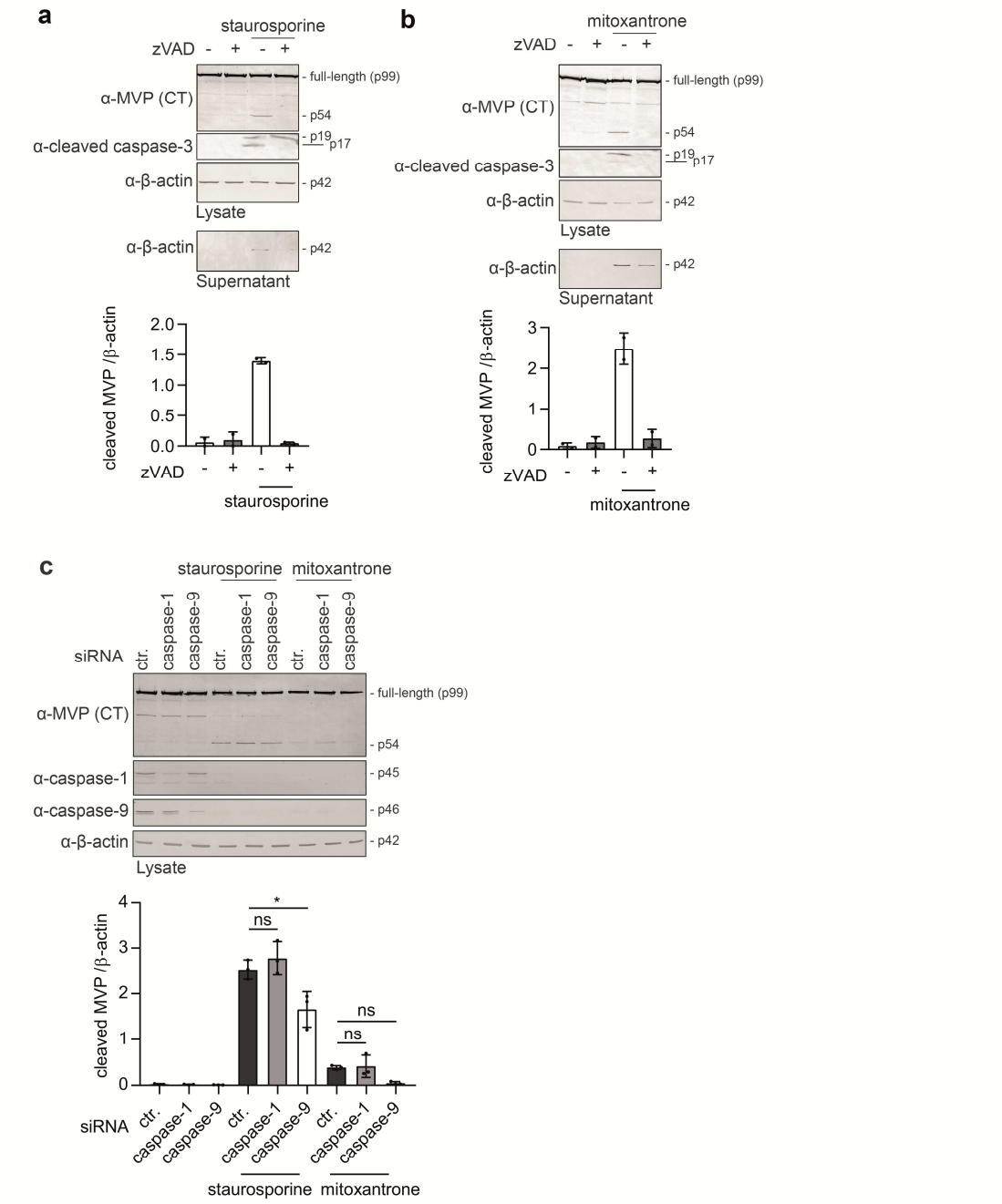

Supplementary Figure S3. Cell death induces MVP cleavage in human primary fibroblasts (HPFs) dependent on caspase-9 expression.

(**a** and **b**) Immunoblot analysis (above) and quantification of the band corresponding to the cleaved MVP fragment (p54) normalized to β-actin (below) of HPFs either untreated, treated with staurosporine (0.5 μM) (**a**) or with mitoxantrone (25 μm) (**b**) for 20 h, after pre-treatment with DMSO (-) or zVAD (10 μM) for 1 h. Graph bars in (**a** and **b**) represent mean ± SD of *n* = 2 independent experiments. (**c**) Immunoblot analysis (above) and quantification of the band

corresponding to the cleaved MVP fragment (p54) normalized to β-actin (below) of HPFs 48 h after transfection with scrambled siRNA (ctr.) or caspase-1 and caspase-9 targeting siRNAs, with either no treatment, treatment with staurosporine (0.5 μM) or with mitoxantrone (25 μM) for 20 h. Graph bars represent mean ± SD of n = 3 independent experiments with one-way analysis of variance (ANOVA) with Dunnet's multiple-comparison test (*$p<0.05$). One representative Western blot from three experiments is shown.

Abbreviations: CT: targeting the carboxy-terminal part; ns: not significant.

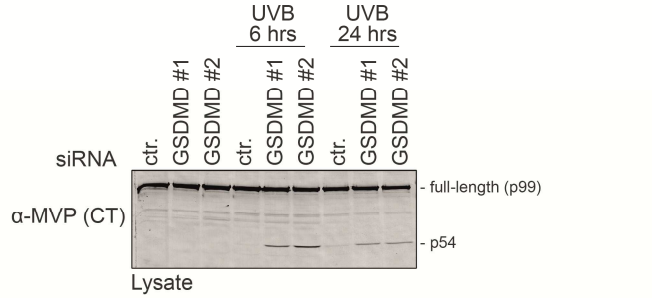

Supplementary Figure S4. Knockdown of GSDMD expression promotes apoptosis and MVP cleavage upon UVB irradiation.

Immunoblot analysis of HPKs (from the same experiments shown in Fig. 1c) 48 h after transfection with scrambled siRNA (ctr.) or GSDMD targeting siRNAs (GSDMD #1 and GSDMD #2) subjected to UVB irradiation (0.0875 J/cm^2) for 6 and 24 h or without treatment (n = 2).

Abbreviations: CT: targeting the carboxy-terminal part.

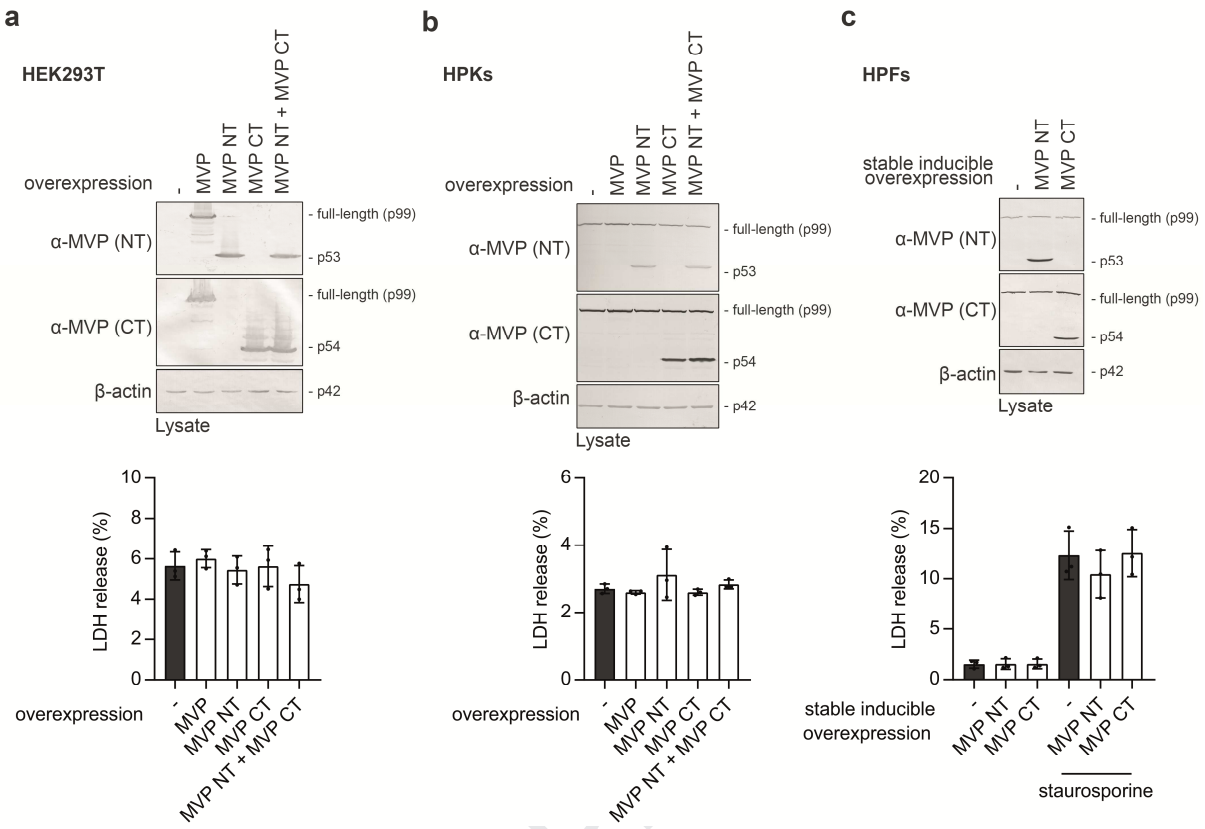

Supplementary Figure S5. Overexpression of MVP fragments does not influence cell death.

Immunoblot analysis (above) and analysis of LDH release (below) of HEK293T cells (**a**) and HPKs (**b**) 24 h after transfection with plasmids encoding either an empty vector (-), or wild-type MVP (MVP), MVP N-terminal fragment (MVP NT), MVP C-terminal fragment (MVP CT) or a combination of the latter. (**c**) Immunoblot analysis (above) and analysis of LDH release (below) of stably genetically modified HPFs treated 20 h with doxycycline (1 µg/ml) to induce expression of either eGFP, MVP N-terminal fragment (MVP NT) or MVP C-terminal fragment (MVP CT) without or with treatment with staurosporine (0.5 µM) for 20 h. Graph bars in (**a** – **c**) represent mean ± SD of a representative experiment (n = 2). One representative Western blot from two experiments is shown.

Abbreviations: NT: targeting the amino-terminal part; CT: targeting the carboxy-terminal part; ns: not significant.

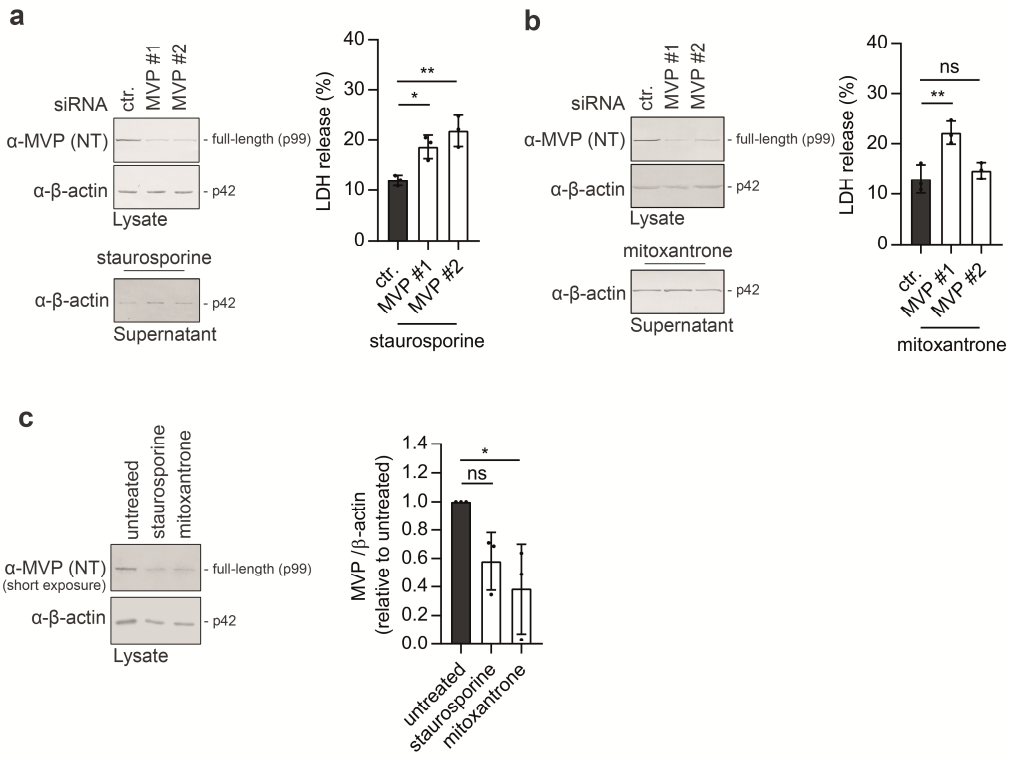

Supplementary Figure S6. MVP is a cytoprotective protein in human primary fibroblasts (HPFs) and its amount is reduced upon induction of apoptosis.

(**a** and **b**) Immunoblot analysis (left) and analysis of LDH release of HPFs 48 h after transfection with scrambled siRNA (ctr.) or MVP targeting siRNAs (MVP #1 and MVP #2) with either treatment with staurosporine (0.5 μM) (**a**) or with mitoxantrone (12.5 μM) (**b**) for 20 h. Graph bars in (**a** and **b**) represent mean ± SEM of *n* = 3 independent experiments with one-way analysis of variance (ANOVA) with Dunnet's multiple-comparison test (*p<0.05, **p<0.01). (**c**) Immunoblot analysis (left) and quantification of the band corresponding to full-length MVP normalized to β-actin and compared to untreated cells (right) of HPFs either untreated, treated with staurosporine (0.5 μM) or with mitoxantrone (12.5 μM) for 20 h. Error bars represent mean ± SD of *n* = 3 independent experiments with one-way analysis of variance (ANOVA) with Dunnet's multiple-comparison test (*=p<0.05). One representative Western blot from three experiments is shown.

Abbreviations: NT: targeting the amino-terminal part: ns: not significant.

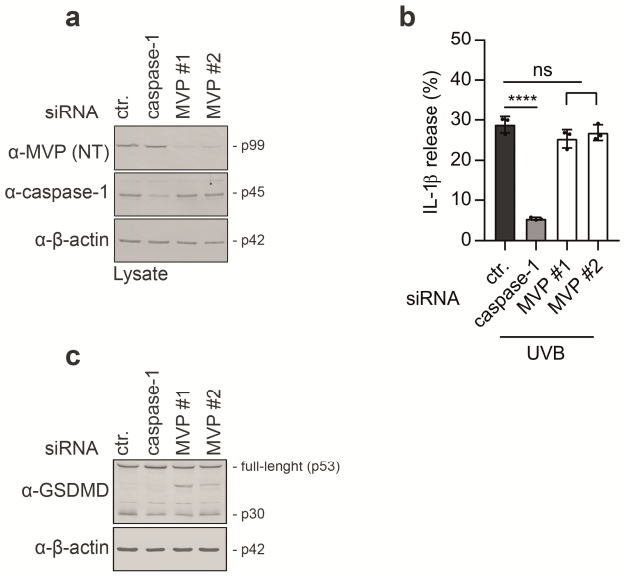

Supplementary Figure S7. MVP expression is not required for inflammasome activation. Immunoblot analysis (**a**, **c**) and analysis of IL-1β release in the supernatant by ELISA (**b**) of HPKs 48 h after transfection with scrambled siRNA (ctr.) or caspase-1 and MVP targeting siRNAs (MVP #1 and MVP #2) and 6 h after exposure to UVB radiation (0.0875 J/cm^2). Percentage of IL-1β release was calculated according to the following formula: IL-1β in the supernatant / (IL-1β in the supernatant + IL-1β in the lysate) × 100. Error bars represent mean ± SEM of n = 3 independent experiments with one-way analysis of variance (ANOVA) with Dunnet's multiple-comparison test (****=p<0.0001).

Abbreviations: NT: targeting the amino-terminal part; ns: not significant.

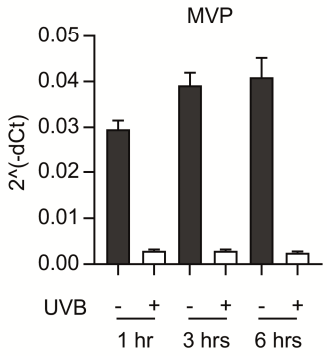

Supplementary Figure S8. MVP mRNA is downregulated upon UVB irradiation.

Quantitative real-time PCR analysis of MVP mRNA expression (normalized to RLP27) in HPKs either UVB-irradiated (0.0875 J/cm^2) or left untreated, and harvested at the indicated time points. Graph bars represent mean ± SD of technical replicates from a single experiment (n = 1).

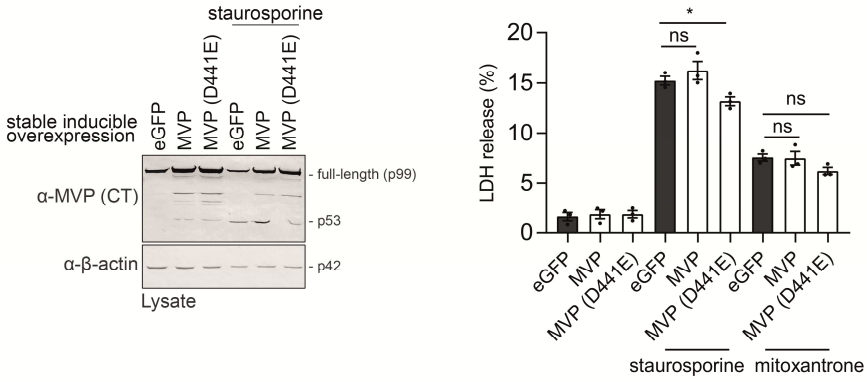

Supplementary Figure S9. Cleavage resistant MVP protects human primary fibroblasts (HPFs) from cell death.

Immunoblot analysis (left) and analysis of LDH release (right) of stably genetically modified HPFs treated for 20 h with doxycycline (1 μg/ml) to induce expression of eGFP, MVP or MVP (D441E) and subjected to either treatment with staurosporine (0.5 μM), mitoxantrone (6.25 μM) for 20 h or left untreated. Graph bars represent mean ± SEM of $n = 3$ independent experiments with two-way analysis of variance (ANOVA) with Turkey's multiple-comparison test (*=$p<0.05$).

Abbreviations: CT: targeting the carboxy-terminal part; ns: not significant.

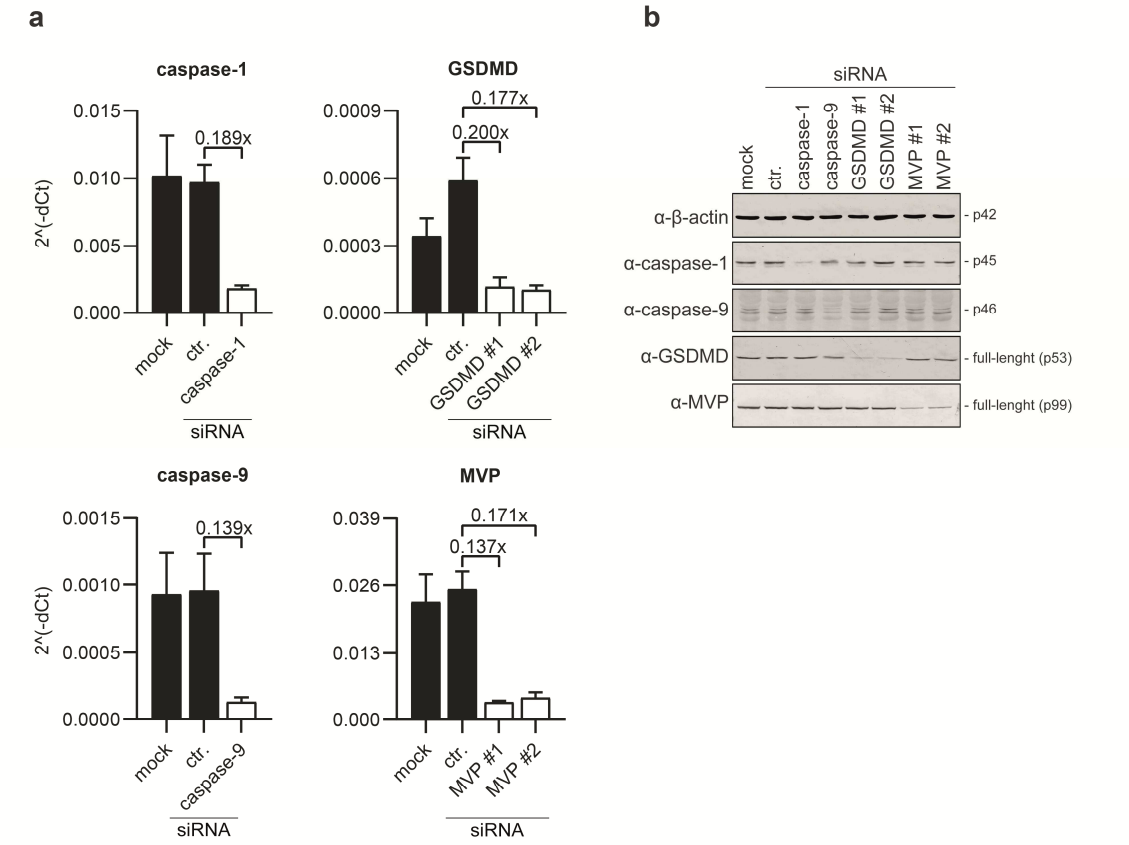

Supplementary Figure S10. Knockdown efficiency of used siRNAs in HPKs.

HPKs were transfected for 48 h with the indicated siRNAs. mRNA and proteins were isolated and analyzed for expression of the indicated genes by quantitative real-time PCR normalized to RPL27 (**a**) or Western Blot (**b**). Fold reduction to ctr. siRNA is indicated (**a**).

REFERENCES

Fenini G, Grossi S, Contassot E, Biedermann T, Reichmann E, French LE, et al. Genome Editing of Human Primary Keratinocytes by CRISPR/Cas9 Reveals an Essential Role of the NLRP1 Inflammasome in UVB Sensing. J Invest Dermatol 2018;138(12):2644-52.

Kockmann T, Carte N, Melkko S, auf dem Keller U. Identification of Protease Substrates in Complex Proteomes by iTRAQ-TAILS on a Thermo Q Exactive Instrument. In: Grant JE, Li H, editors. Analysis of Post-Translational Modifications and Proteolysis in Neuroscience. New York, NY: Springer New York; 2016. p. 187-207.

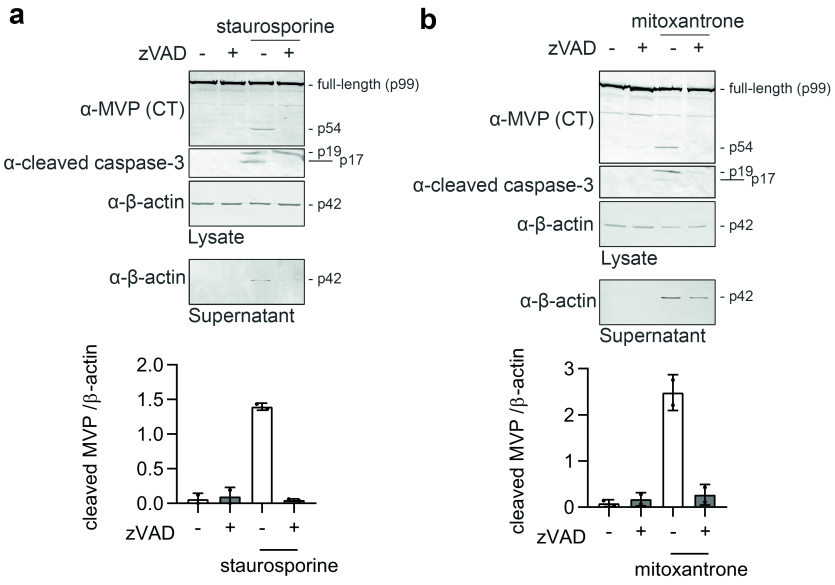
a
staurosporine
zVAD - + - +
α-MVP (CT)
- full-length (p99)
- p54
α-cleaved caspase-3
- p19 p17
α-β-actin
- p42
Lysate
α-β-actin
- p42
Supernatant
cleaved MVP /β-actin
2.0
1.5
1.0
0.5
0.0
zVAD - + - +
staurosporine
b
mitoxantrone
zVAD - + - +
α-MVP (CT)
- full-length (p99)
- p54
α-cleaved caspase-3
- p19 p17
α-β-actin
- p42
Lysate
α-β-actin
- p42
Supernatant
cleaved MVP /β-actin
3
2
1
0
zVAD - + - +
mitoxantrone

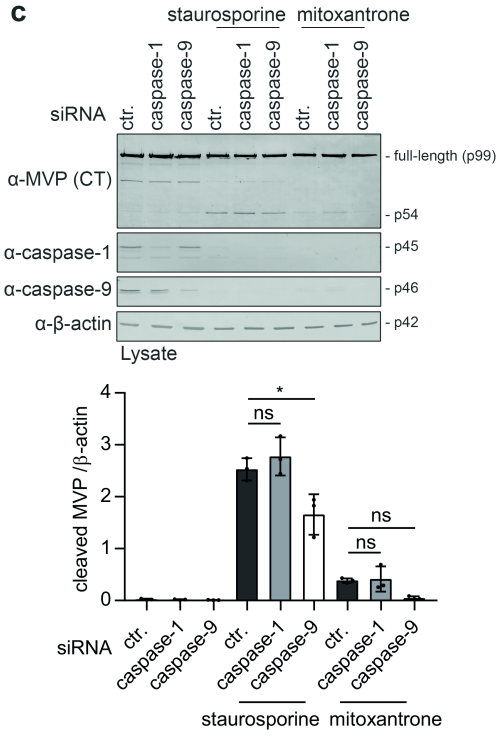
c
staurosporine mitoxantrone
siRNA ctr. caspase-1 caspase-9 ctr. caspase-1 caspase-9 ctr. caspase-1 caspase-9
α-MVP (CT)
- full-length (p99)
- p54
α-caspase-1
- p45
α-caspase-9
- p46
α-β-actin
- p42
Lysate
cleaved MVP /β-actin
4
3
2
1
0
*
ns
ns
ns
siRNA ctr. caspase-1 caspase-9 ctr. caspase-1 caspase-9 ctr. caspase-1 caspase-9
staurosporine mitoxantrone

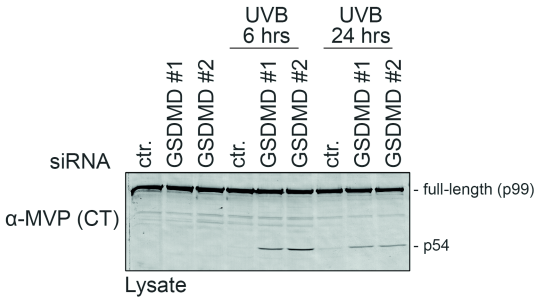

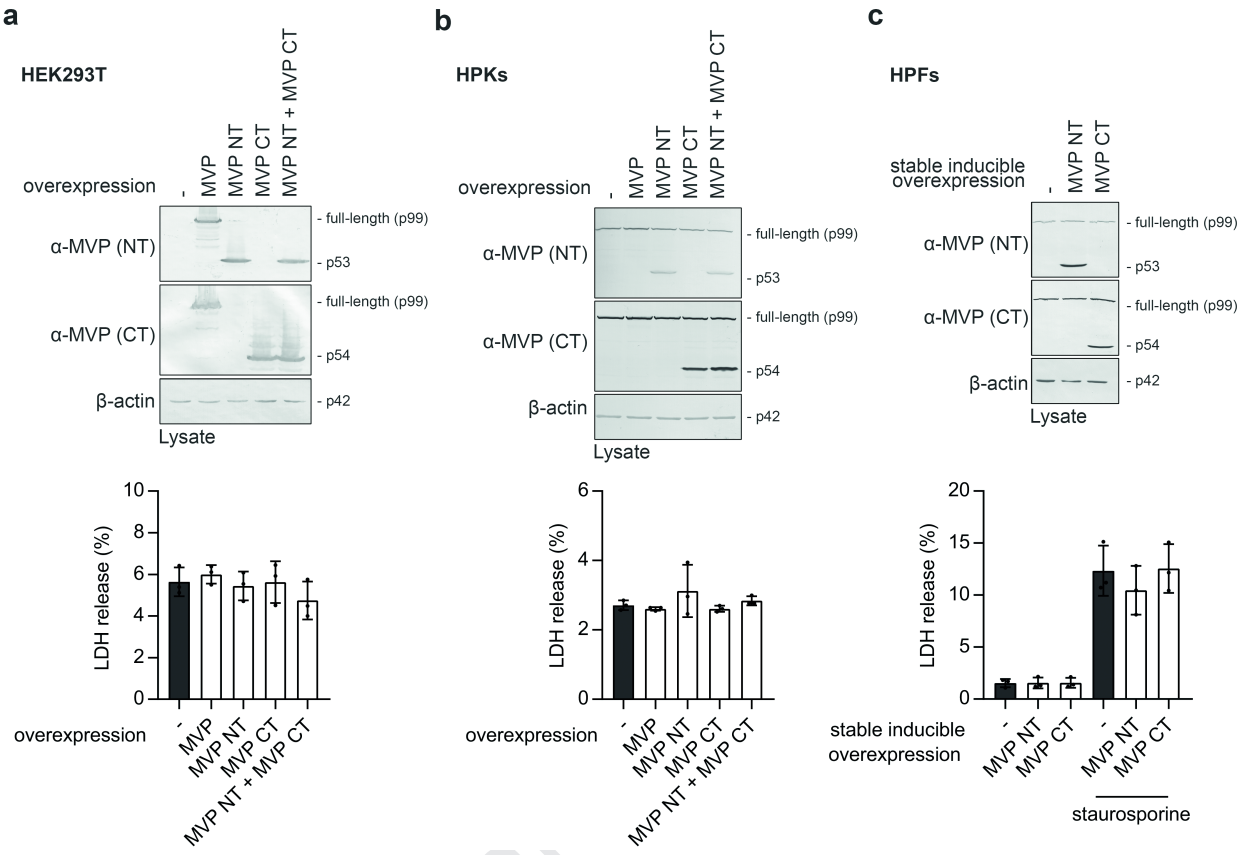
a
HEK293T
overexpression
-
MVP
MVP NT
MVP CT
MVP NT + MVP CT
α-MVP (NT)
- full-length (p99)
- p53
α-MVP (CT)
- full-length (p99)
- p54
β-actin
- p42
Lysate
LDH release (%)
overexpression
b
HPKs
c
HPFs
stable inducible overexpression
staurosporine

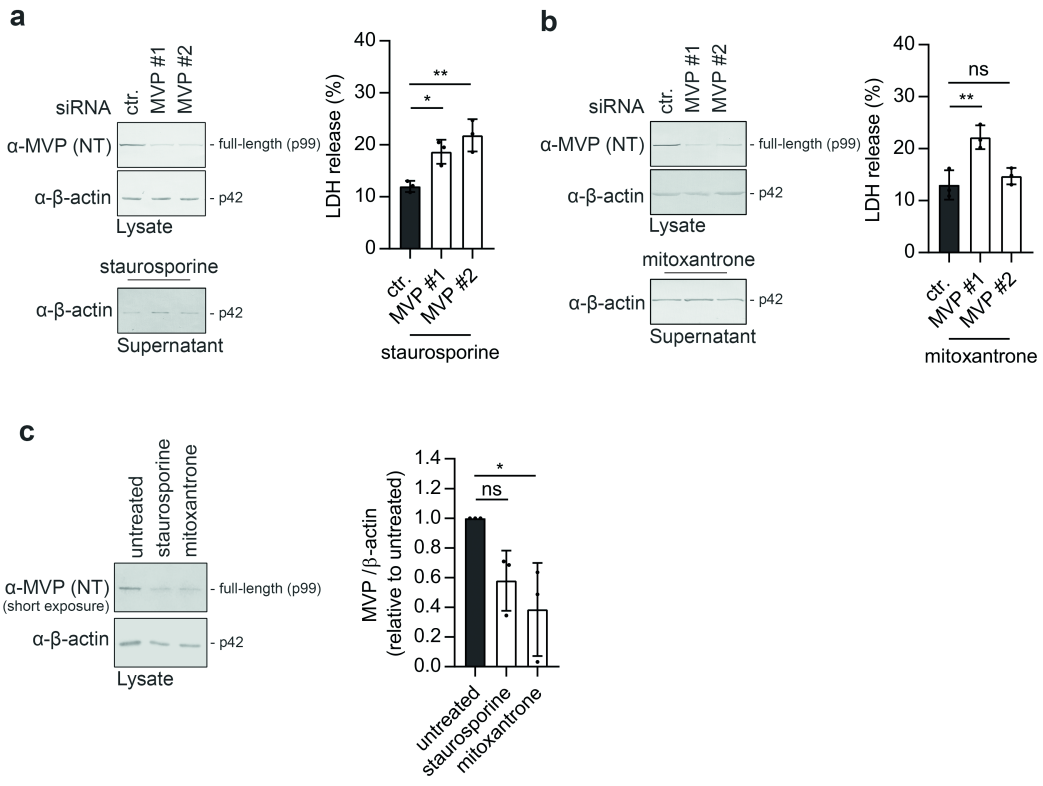
a
siRNA
ctr.
MVP #1
MVP #2
α-MVP (NT)
- full-length (p99)
α-β-actin
- p42
Lysate
staurosporine
α-β-actin
- p42
Supernatant
LDH release (%)
40
30
20
10
0
**
*
ctr.
MVP #1
MVP #2
staurosporine
b
siRNA
ctr.
MVP #1
MVP #2
α-MVP (NT)
- full-length (p99)
α-β-actin
- p42
Lysate
mitoxantrone
α-β-actin
- p42
Supernatant
LDH release (%)
40
30
20
10
0
ns
**
ctr.
MVP #1
MVP #2
mitoxantrone
c
untreated
staurosporine
mitoxantrone
α-MVP (NT)
(short exposure)
- full-length (p99)
α-β-actin
- p42
Lysate
MVP /β-actin
(relative to untreated)
1.4
1.2
1.0
0.8
0.6
0.4
0.2
0.0
*
ns
untreated
staurosporine
mitoxantrone

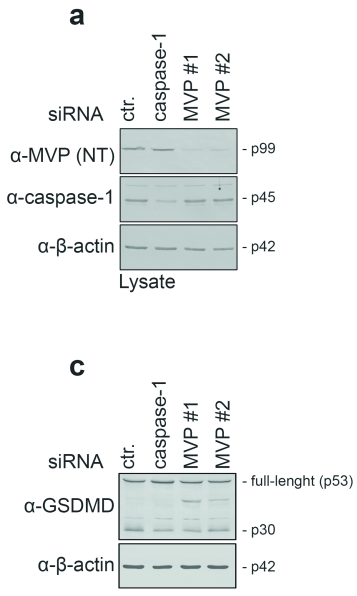

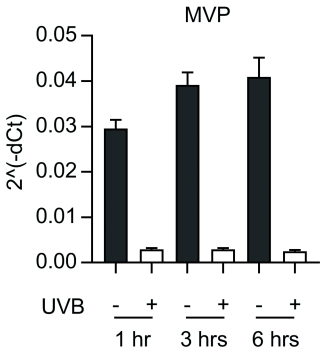

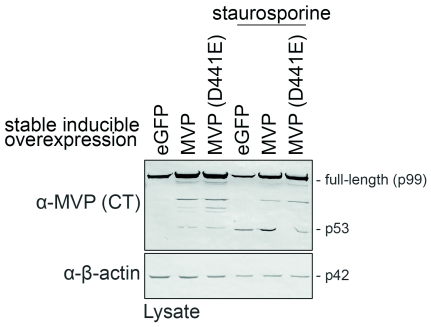

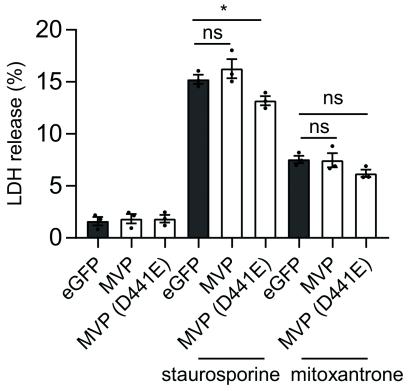

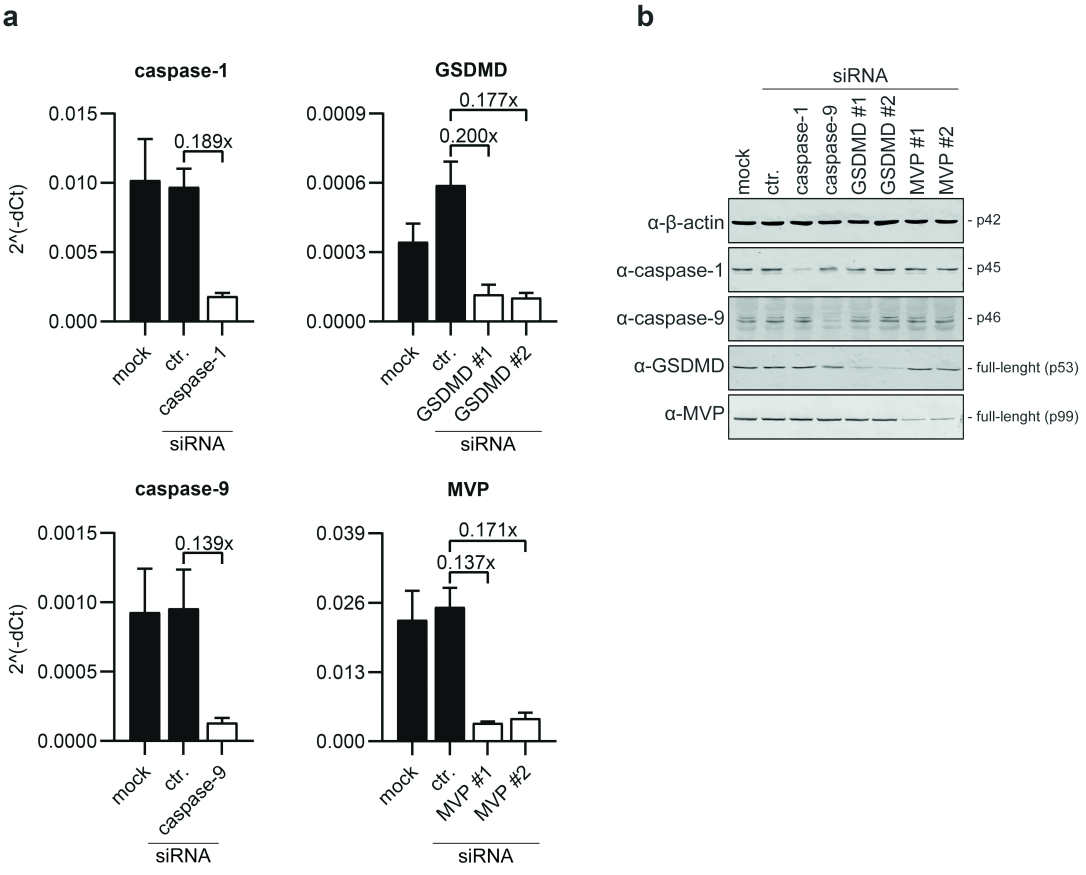
a
caspase-1
0.189x
2^(-dCt)
0.015
0.010
0.005
0.000
mock
ctr.
caspase-1
siRNA
GSDMD
0.177x
0.200x
0.0009
0.0006
0.0003
0.0000
mock
ctr.
GSDMD #1
GSDMD #2
siRNA
caspase-9
0.139x
2^(-dCt)
0.0015
0.0010
0.0005
0.0000
mock
ctr.
caspase-9
siRNA
MVP
0.171x
0.137x
0.039
0.026
0.013
0.000
mock
ctr.
MVP #1
MVP #2
siRNA
b
siRNA
mock
ctr.
caspase-1
caspase-9
GSDMD #1
GSDMD #2
MVP #1
MVP #2
α-β-actin
- p42
α-caspase-1
- p45
α-caspase-9
- p46
α-GSDMD
- full-lenght (p53)
α-MVP
- full-lenght (p99)